Supplement of Characterizing Lightning NO_x Production in the Ebro Valley with MTG-LI and LMA Observations

Francisco J. Pérez-Invernón[1], Francisco J. Gordillo-Vázquez[1], Oscar van der Velde[2], Joan Montanyà[2], Jesús Alberto López Trujillo[2], Nicolau Pineda[3], Diego Loyola[4], Sora Seo[4], Christoph Knote[5], Alexandre O. Fierro[6], and Heidi Huntrieser[7]

[1]Instituto de Astrofísica de Andalucía (IAA), CSIC, PO Box 3004, 18080 Granada, Spain
[2]Lightning Research Group, Polytechnic University of Catalonia, Terrassa, Spain
[3]Meteorological Service of Catalonia
[4]Deutsches Zentrum für Luft- und Raumfahrt, Methodik der Fernerkundung, Wessling, Germany
[5]Chair of Model-Based Environmental Exposure Science, Faculty of Medicine, University of Augsburg, Augsburg, Germany
[6]Metocean Team, I&E Engineering, BP Exploration and Operating Company, Ltd., Sunbury, UK.
[7]Deutsches Zentrum für Luft- und Raumfahrt, Institut für Physik der Atmosphäre, Oberpfaffenhofen, Germany

Correspondence: Francisco J. Pérez-Invernón (fjpi@iaa.es)

1 Introduction

The candidate dates selected for analysis are presented in Table S1. Table S2 shows the basic measurements for each analyzed date.

Figures S1 to S51 show the analysis of simulation results, TROP-DLR products, lightning measurements and calculated $V_{tropNOx}$ of the cases not shown in the main part of the manuscript.

Figure S52 shows pixel-based $\mathbf{V}_{tropLNOx}$ versus average lightning characteristics computed across all pixels included in the 18 analyzed dates. The included linear fittings and binned data indicates positive relationships between the $V_{tropLNOx}$ and the analyzed lightning characteristics. Figures S53 and S54 are equivalent to Figures 5 and 6 of the main manuscript, but using τ = 3 h instead of τ = 5 h. These figures show that there are not significant differences in the obtained correlations between the LNO_x PE and the main lightning characteristics when using a different value for τ. In fact, the majority of the positive correlations are stronger when using τ = 3 h.

Figure S55 shows the analysis of the influence of the background-NO_x estimate in the obtained relationships.

2 Tables

Date	Flashes	Selected	Main reason for non-selection	Selected ROI
2024-07-06	5752	Yes	-	42.0°N-42.9°N, 0.0°E-3.5°E
2024-07-21	13359	Yes	-	42.0°N-42.9°N, 0.0°E-4.5°E
2024-08-02	3870	Yes	-	39.7°N-41.6°N, 2°W-1.5°E
2024-08-13	11058	Yes	-	42.75°N-42.5°N, 0.0°E-3.5°E
2024-08-14	39078	Yes	-	41.5°N-42.5°N, 2.0°E-3.5°E
2024-08-22	2144	No	Only 479 flashes withint the LMA area	-
2024-08-23	2729	Yes	-	39.5°N-41.0°N, 3.5°W-0.0°E
2024-08-25	1068	Yes	-	40.0°N-42.0°N, 3.5°W-0.5°E
2024-09-01	1004	No	Activity centered out of the LMA area (Northwest)	-
2024-09-02	7404	Yes	-	40.0°N-41.5°N, 2.5°W- 0.5°W
2024-09-03	45558	Yes	-	39.5°N-42.9°N, -1.2°W-3.5°E
2024-09-04	28700	No	Activity centered out of the LMA area (Southeast Balearic Sea)	-
2024-09-06	3312	No	Activity centered out of the LMA area (Northwest)	-
2024-09-21	2970	Yes	-	40.5°N-42.9°N, 2.5°W- 0.3°W
2024-09-22	825	No	Activity centered out of the LMA area (Northwest and Southeast Balearic Sea)	-
2024-09-23	7503	No	Age larger than 3.5 hours	-
2024-09-24	11088	No	Activity centered out of the LMA area (Southeast Balearic Sea)	-
2024-10-15	5416	Yes	-	39.7°N-41.5°N, 1.5°W-0.0°E
2024-10-17	12665	No	The LNOx advected outside the LMA area	-
2024-10-26	7194	No	Activity centered out of the LMAarea (Southeast Balearic Sea)	-
2024-10-29	5459	No	Activity centered out of the LMA area (Southwest)	-
2024-10-30	9020	No	Activity centered out of the LMA area (Northwest)	-
2024-10-31	5139	Yes	-	40.0°N-42.0°N, 1.5°W-2.0°E
2024-11-01	4507	Yes	-	39.9°N-41.5°N, 0.5°W-4.5°E
2024-11-04	2396	No	Age larger than 3.5 hours	-
2024-11-12	739	No	Activity centered out of the LMA area (Southeast Balearic Sea)	-
2024-11-13	2603	Yes	-	39.0°N-41.5°N, 1.3°W-3.2°E
2025-04-14	3946	No	Activity centered out of the LMA area (Southwest)	-
2025-04-15	1556	Yes	-	41.5°N-42.9°N, 1.0°E-4.0°E
2025-04-19	5592	Yes	-	39.5°N-42.9°N, 1.5°W-2.5°E
2025-04-22	950	No	Only 531 flashes within the LMA area	
2025-04-26	1436	Yes	-	41.7°N-42.9°N, 0.0°E-3.2°
2025-05-02	5823	No	Activity centered out of the LMA area (West)	-
2025-05-03	1199	No	Activity centered out of the LMA area (North and South)	-
2025-05-04	3753	Yes	-	40.5°N-42.0°N, 1.0°W-1.5°E

Table S1. Date candidates with at least 650 flashes reported by MTG-LI between 7:00 and 14:00 within 39.5°N and 42.9°N latitude, and -1.5°W and 4.5°E longitude. Reasons for non-selection, where applicable, are included. The selected Region of Interest (ROI) is indicated.

Date	Orbit	Flashes (MTG-LI)	Flashes (LMA)	CG Flashes (LLS-SMC)	Age MTG-LI (h)	Age LMA (h)	OCP (hPa)	Valid pixels	Pixels with MTG-LI flash	Pixels with LMA flash
2024-07-06	34875	803	1917	184	0.72	0.49	425.02	154	23	33
2024-07-21	35087	11250	26583	2062	3.38	3.45	469.21	331	153	149
2024-08-02	35258	1736	11313	186	0.63	0.61	337.04	260	94	102
2024-08-13	35414	6653	20296	995	1.52	1.50	365.64	573	219	237
2024-08-14	35428	845	2170	110	0.33	0.32	385.97	80	45	36
2024-08-23	35555	676	1823	65	0.68	0.73	369.89	154	36	42
2024-08-25	35584	752	4100	24	1.82	1.18	323.07	366	85	96
2024-09-02	35697	2885	3896	55	0.65	0.55	369.79	174	80	65
2024-09-03	35711	25929	56203	7622	1.54	1.41	375.85	1614	675	711
2024-09-21	35967	2560	4066	190	1.08	1.01	434.87	657	136	128
2024-10-15	36307	1400	2854	157	0.95	0.78	412.91	284	35	31
2024-10-31	36534	2787	7250	1446	2.30	2.21	341.87	637	233	322
2024-11-01	36549	1959	2997	1166	2.24	2.58	385.81	372	190	226
2024-11-13	36719	1682	2199	261	2.09	2.14	434.51	1109	101	114
2025-04-15	38890	1086	1628	162	1.21	1.27	453.89	256	43	38
2025-04-19	38946	4906	7979	1905	1.69	1.62	493.99	340	146	159
2025-04-26	39046	1318	1699	377	1.65	1.65	499.34	89	31	34
2025-05-04	39159	1439	3688	153	0.68	0.69	384.22	509	79	59

Table S2. Analyzed dates, orbits, total number flashes detected by MTG-LI, LMA and CG flashes detected by LSS-SMC up to 5 h before the overpass of TROPOMI, average flash age according to MTG-LI and LMA, average OCP in TROPOMI pixels satisfying the DCC, total number of valid TROPOMI pixels satisfying the DCC, and total number of TROPOMI pixels with MTG-LI or LMA flashes satisfying the DCC.

3 Figures

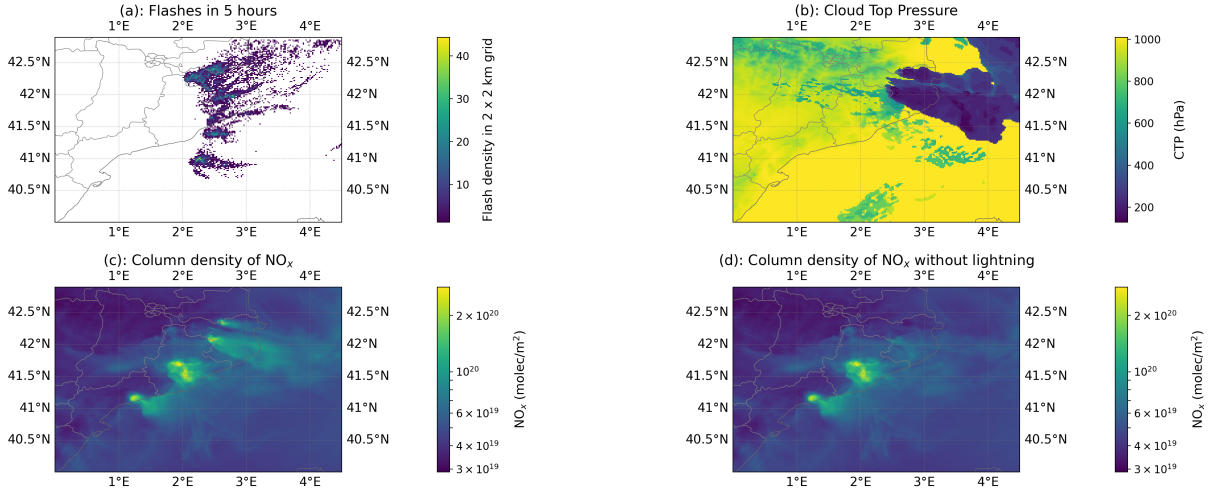

Figure S1. Simulation results for 21 July 2024 at 12:30 UTC, focused on the region of interest. (a): Assimilated lightning flashes between 07:30 and 12:30 UTC reported by MTG-LI. (b): Cloud Top Pressure (CTP). (c): Vertical Column Density of NO_x. (d): Vertical column density of NO_x in the simulation without fresh LNO_x, i.e., with LNO_x deactivated after 07:00 UTC.

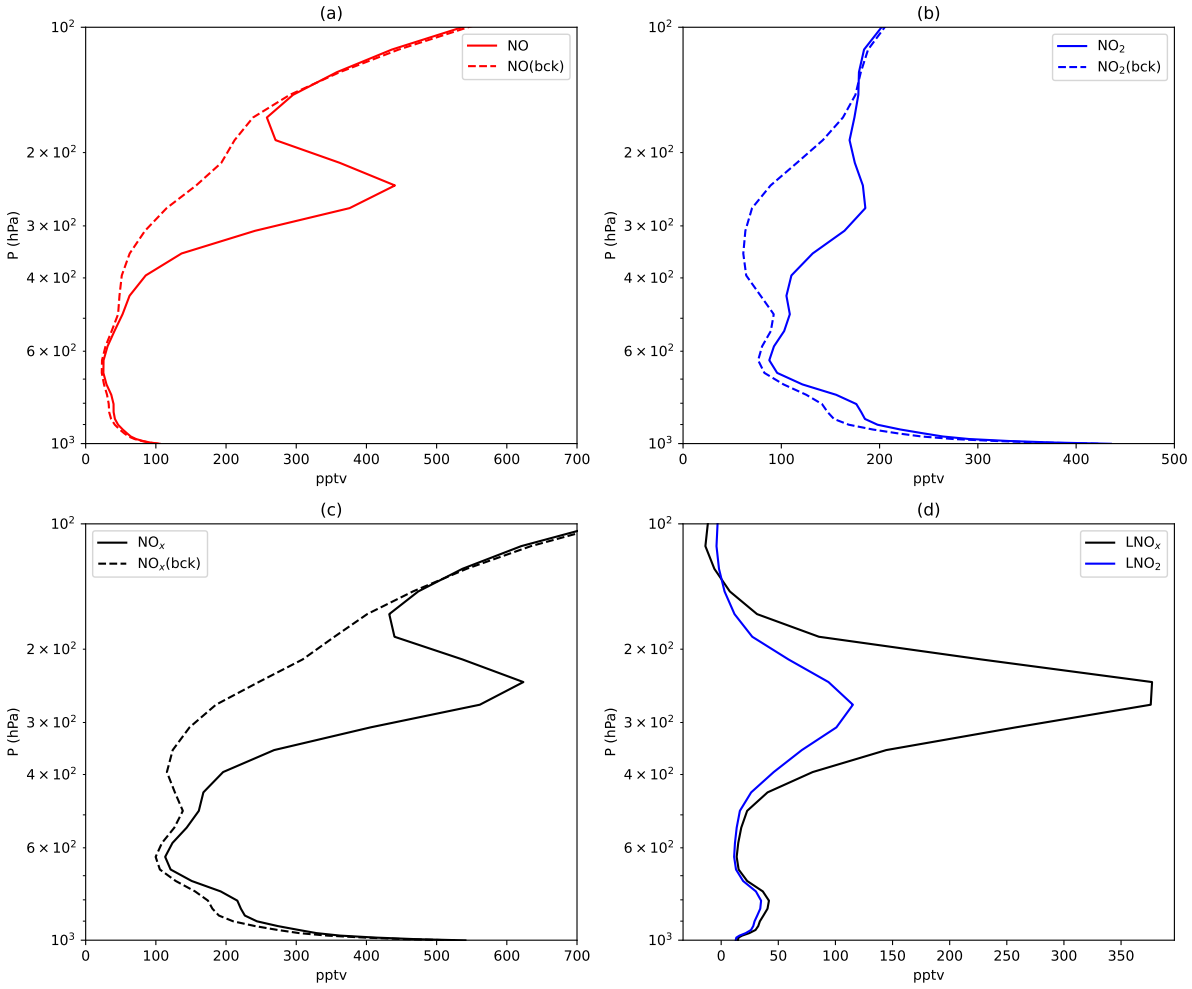

Figure S2. Vertical mixing ratio profiles of NO (a), NO_2 (b), NO_x (c), LNO_x and LNO_2 (d) extracted from WRF-CHEM simulations with (solid lines) and without (dashed lines) fresh LNO_x on 21 July 2024 at 12:30 UTC (close to the TROPOMI overpass (background: bck)).

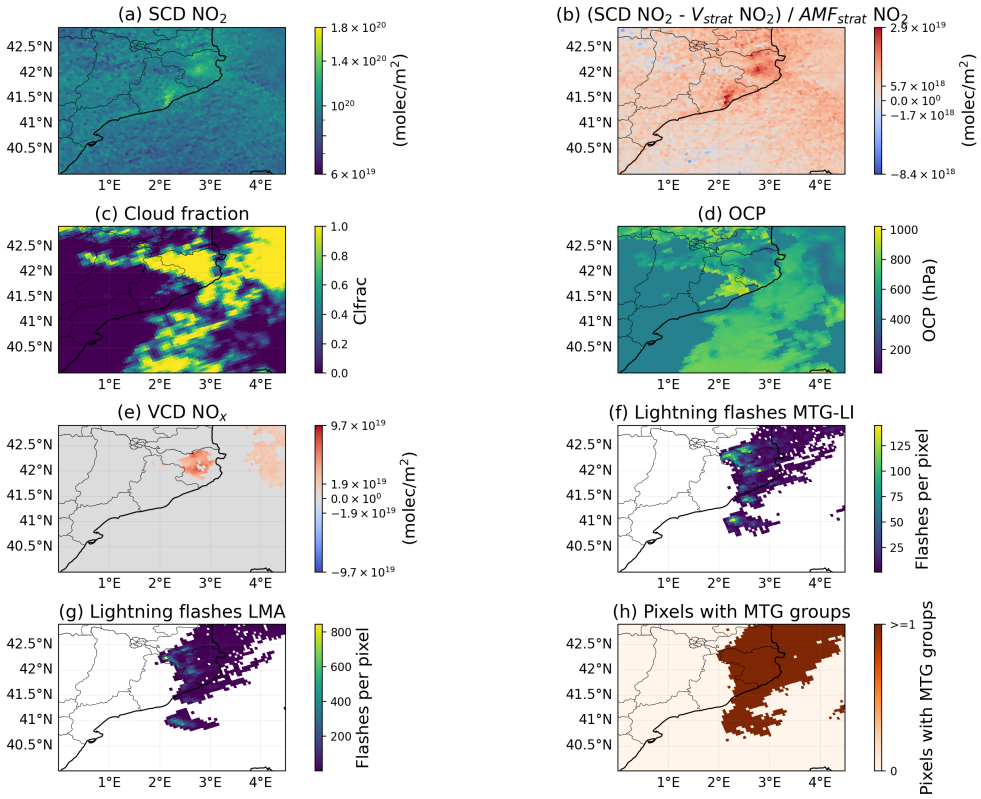

Figure S3. TROP-DLR product of orbit 35087, MTG-LI and LMA lightning data for the case 21 July 2024. (a): Slant Column Density (SCD) of NO_2 provided by the TROP-DLR NO_2 research product. (b): SCD NO_2 minus the stratospheric vertical column density and divided to the stratospheric air mass factor of NO_2 obtained from the TROP-DLR NO_2 research product. (c) and (d): Cloud Fraction (CF) and Optical Centroid Pressure (OCP) from the TROP-DLR NO_2 research product, respectively. (e): VCD of NO_x ($V_{tropNOx}$) over pixels satisfying the DCC. (f) and (g): Lightning flashes during the 5 h period per TROPOMI pixel before the TROPOMI overpass reported by MTG-LI and the LMA, respectively. (h): TROPOMI pixels containing at least one lightning group detected by MTG-LI.

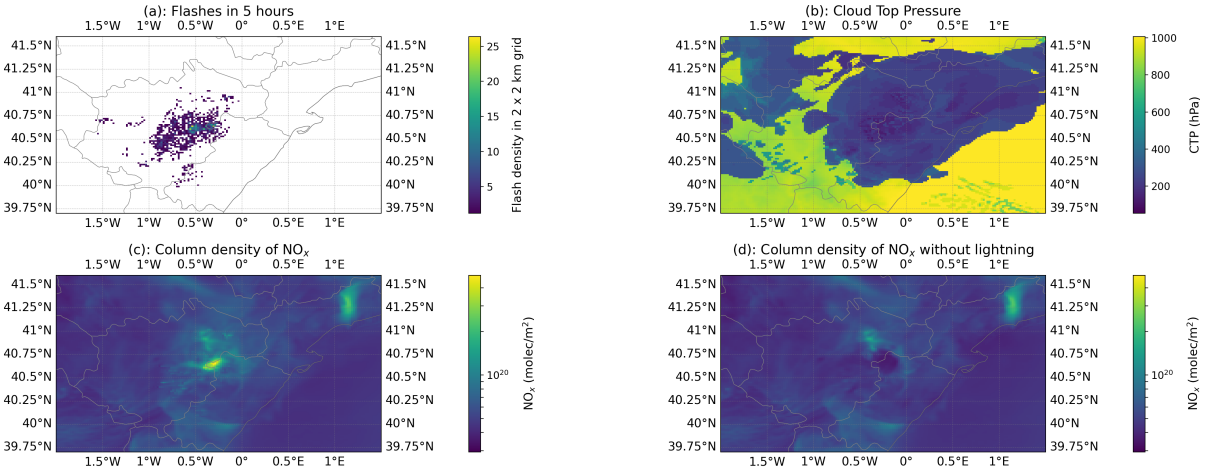

Figure S4. Simulation results for 2 August 2024 at 13:50 UTC, focused on the region of interest. (a): Assimilated lightning flashes between 08:50 and 13:50 UTC reported by MTG-LI. (b): Cloud Top Pressure (CTP). (c): Vertical Column Density of NO_x. (d): Vertical column density of NO_x in the simulation without fresh LNO_x, i.e., with LNO_x deactivated after 07:00 UTC.

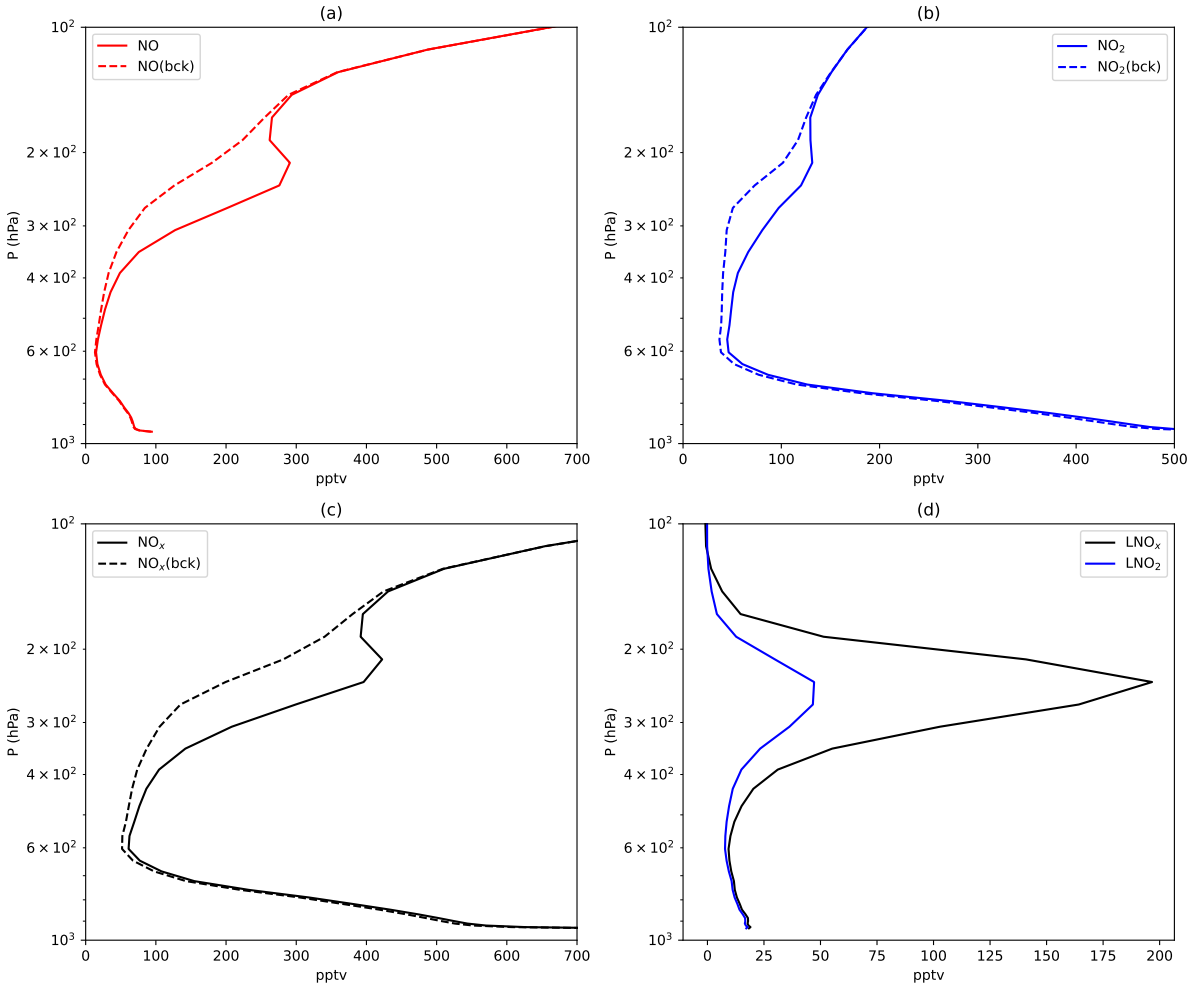

Figure S5. Vertical mixing ratio profiles of NO (a), NO_2 (b), NO_x (c), LNO_x and LNO_2 (d) extracted from WRF-CHEM simulations with (solid lines) and without (dashed lines) fresh LNO_x on 2 August 2024 at 13:50 UTC (close to the TROPOMI overpass (background: bck)).

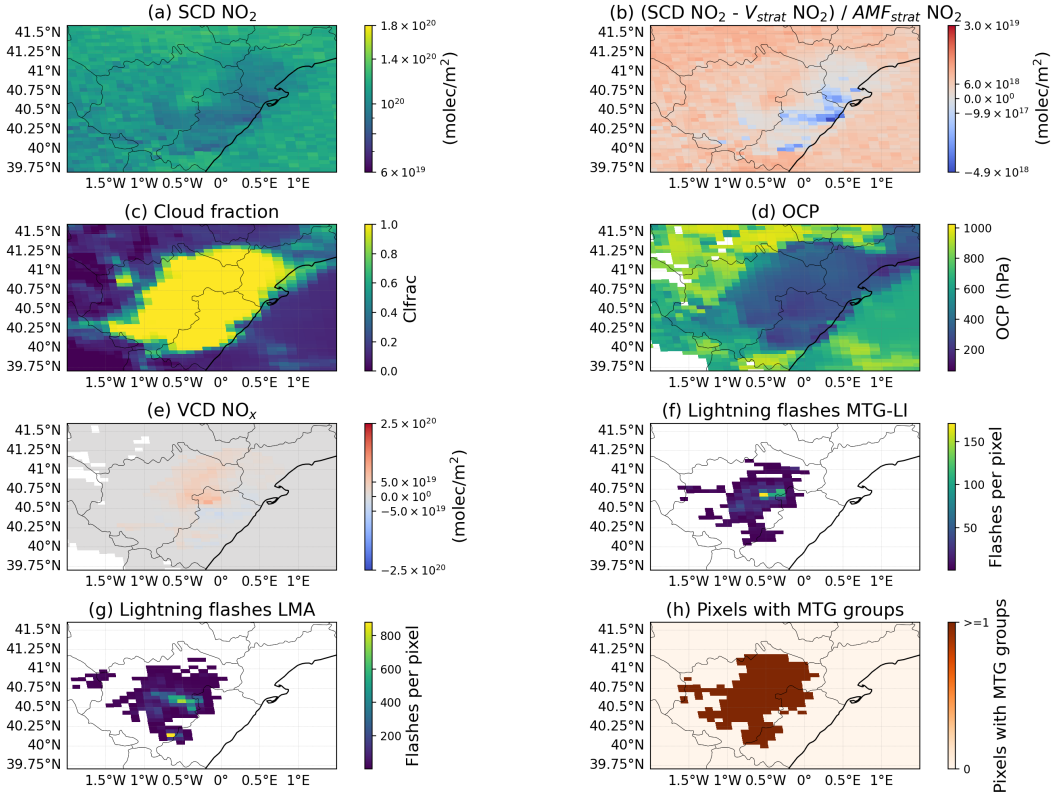

Figure S6. TROP-DLR product of orbit 35258, MTG-LI and LMA lightning data for the case 2 August 2024. (a): Slant Column Density (SCD) of NO_2 provided by the TROP-DLR NO_2 research product. (b): SCD NO_2 minus the stratospheric vertical column density and divided to the stratospheric air mass factor of NO_2 obtained from the TROP-DLR NO_2 research product. (c) and (d): Cloud Fraction (CF) and Optical Centroid Pressure (OCP) from the TROP-DLR NO_2 research product, respectively. (e): VCD of NO_x ($V_{tropNOx}$) over pixels satisfying the DCC. (f) and (g): Lightning flashes during the 5 h period per TROPOMI pixel before the TROPOMI overpass reported by MTG-LI and the LMA, respectively. (h): TROPOMI pixels containing at least one lightning group detected by MTG-LI.

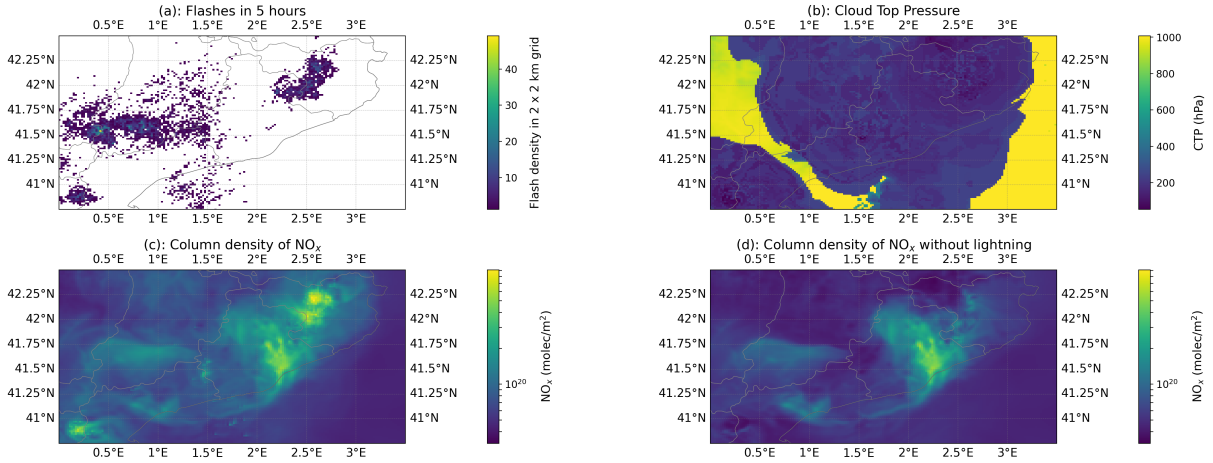

Figure S7. Simulation results for 13 August 2024 at 13:40 UTC, focused on the region of interest. (a): Assimilated lightning flashes between 08:40 and 13:40 UTC reported by MTG-LI. (b): Cloud Top Pressure (CTP). (c): Vertical Column Density of NO_x. (d): Vertical column density of NO_x in the simulation without fresh LNO_x, i.e., with LNO_x deactivated after 07:00 UTC.

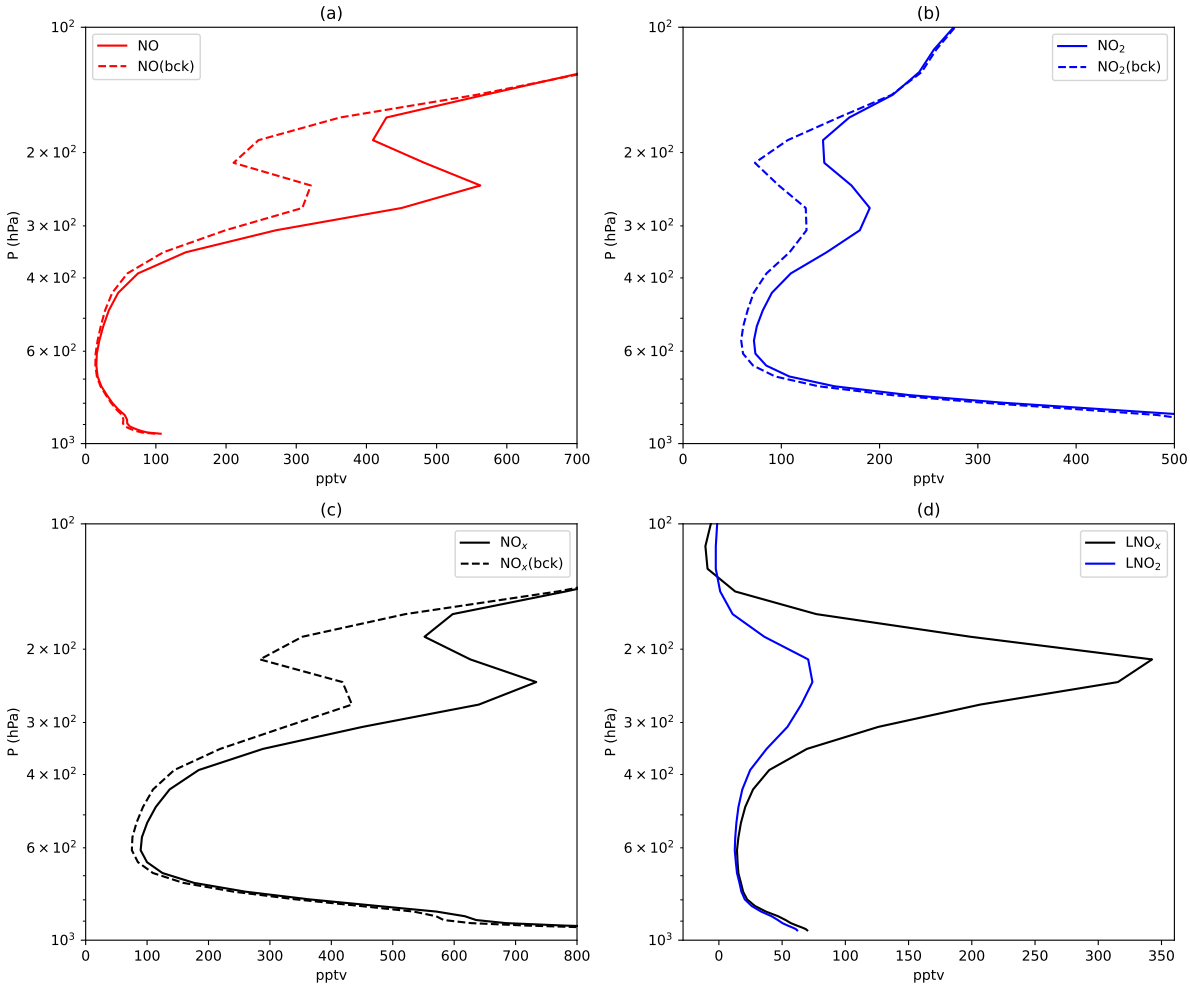

Figure S8. Vertical mixing ratio profiles of NO (a), NO_2 (b), NO_x (c), LNO_x and LNO_2 (d) extracted from WRF-CHEM simulations with (solid lines) and without (dashed lines) fresh LNO_x on 13 August 2024 at 13:40 UTC (close to the TROPOMI overpass (background: bck)).

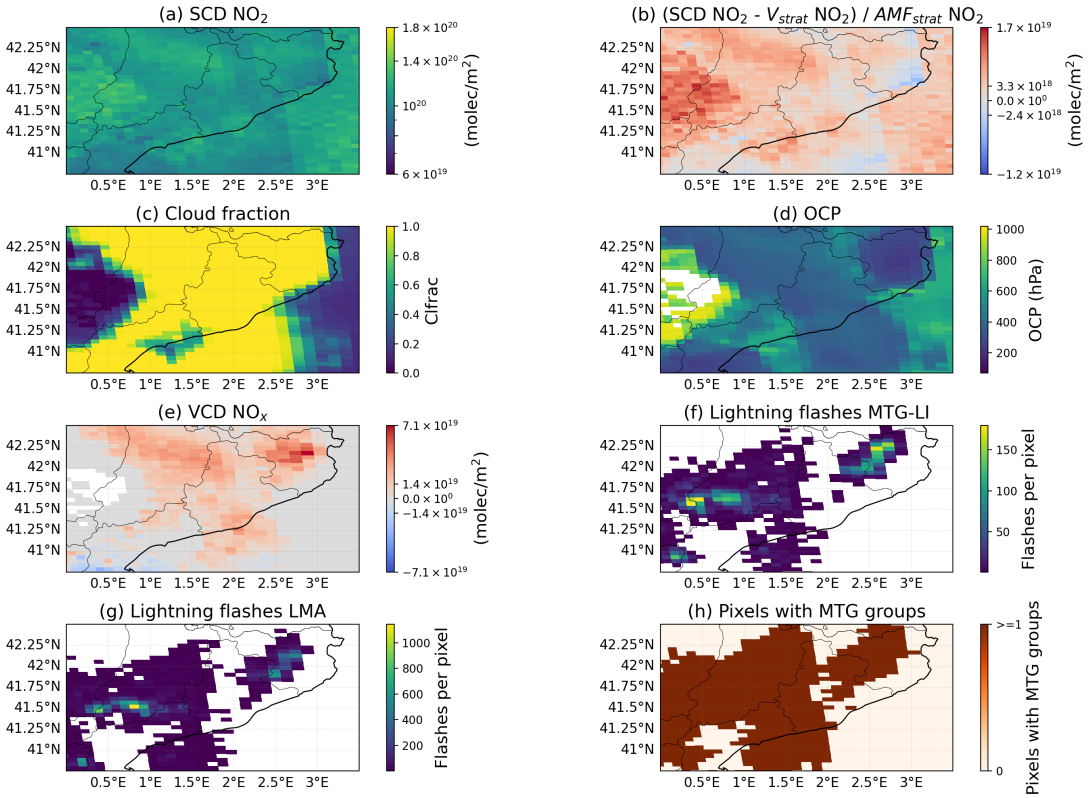

Figure S9. TROP-DLR product of orbit 35414, MTG-LI and LMA lightning data for the case 13 August 2024. (a): Slant Column Density (SCD) of NO_2 provided by the TROP-DLR NO_2 research product. (b): SCD NO_2 minus the stratospheric vertical column density and divided to the stratospheric air mass factor of NO_2 obtained from the TROP-DLR NO_2 research product. (c) and (d): Cloud Fraction (CF) and Optical Centroid Pressure (OCP) from the TROP-DLR NO_2 research product, respectively. (e): VCD of NO_x ($V_{tropNOx}$) over pixels satisfying the DCC. (f) and (g): Lightning flashes during the 5 h period per TROPOMI pixel before the TROPOMI overpass reported by MTG-LI and the LMA, respectively. (h): TROPOMI pixels containing at least one lightning group detected by MTG-LI.

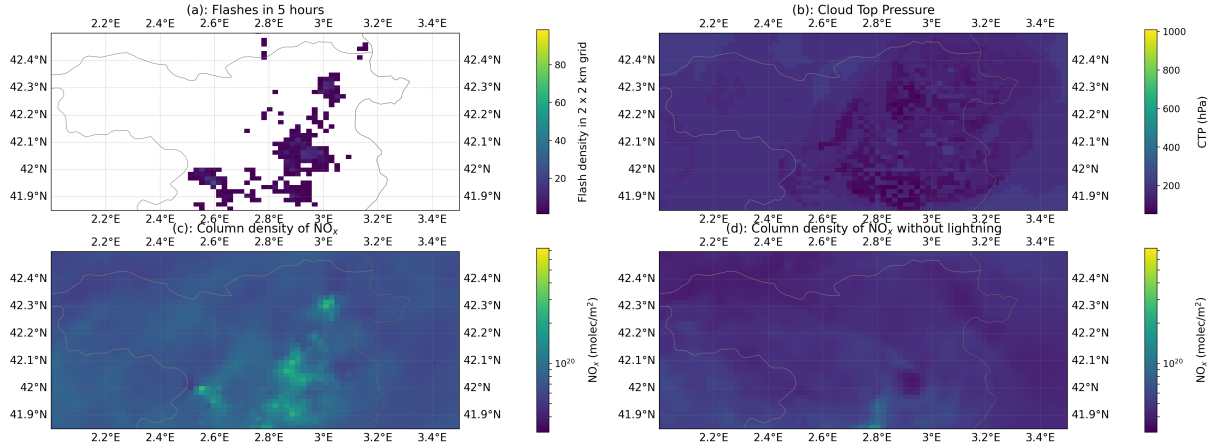

Figure S10. Simulation results for 14 August 2024 at 13:20 UTC, focused on the region of interest. (a): Assimilated lightning flashes between 08:20 and 13:20 UTC reported by MTG-LI. (b): Cloud Top Pressure (CTP). (c): Vertical Column Density of NO_x. (d): Vertical column density of NO_x in the simulation without fresh LNO_x, i.e., with LNO_x deactivated after 07:00 UTC.

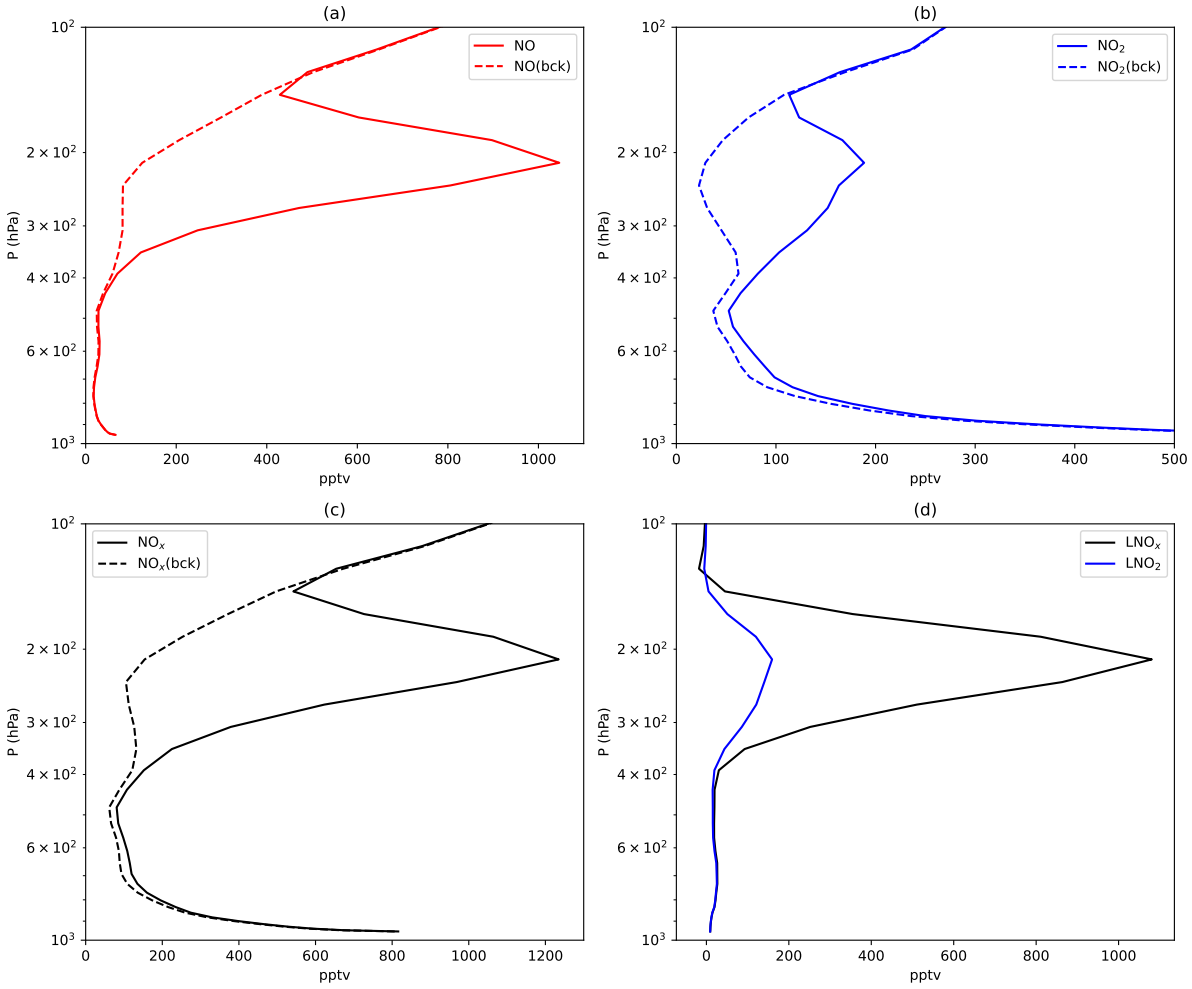

Figure S11. Vertical mixing ratio profiles of NO (a), NO_2 (b), NO_x (c), LNO_x and LNO_2 (d) extracted from WRF-CHEM simulations with (solid lines) and without (dashed lines) fresh LNO_x on 14 August 2024 at 13:20 UTC (close to the TROPOMI overpass (background: bck)).

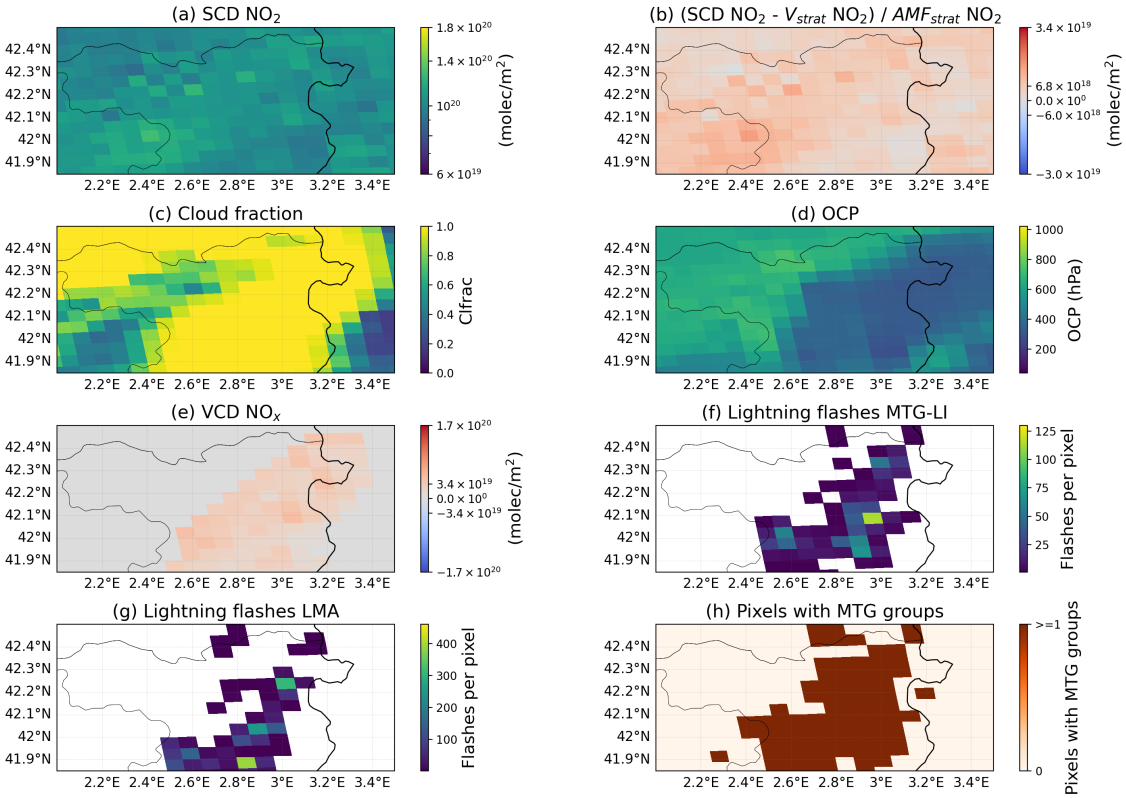

Figure S12. TROP-DLR product of orbit 35428, MTG-LI and LMA lightning data for the case 14 August 2024. (a): Slant Column Density (SCD) of NO_2 provided by the TROP-DLR NO_2 research product. (b): SCD NO_2 minus the stratospheric vertical column density and divided to the stratospheric air mass factor of NO_2 obtained from the TROP-DLR NO_2 research product. (c) and (d): Cloud Fraction (CF) and Optical Centroid Pressure (OCP) from the TROP-DLR NO_2 research product, respectively. (e): VCD of NO_x ($V_{tropNOx}$) over pixels satisfying the DCC. (f) and (g): Lightning flashes during the 5 h period per TROPOMI pixel before the TROPOMI overpass reported by MTG-LI and the LMA, respectively. (h): TROPOMI pixels containing at least one lightning group detected by MTG-LI.

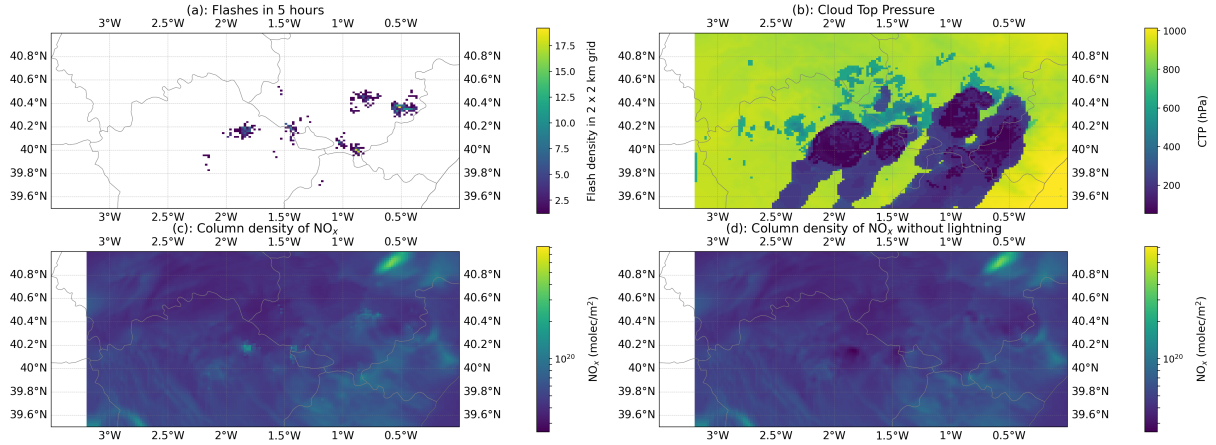

Figure S13. Simulation results for 23 August 2024 at 12:10 UTC, focused on the region of interest. (a): Assimilated lightning flashes between 07:10 and 12:10 UTC reported by MTG-LI. (b): Cloud Top Pressure (CTP). (c): Vertical Column Density of NO_x. (d): Vertical column density of NO_x in the simulation without fresh LNO_x, i.e., with LNO_x deactivated after 07:00 UTC.

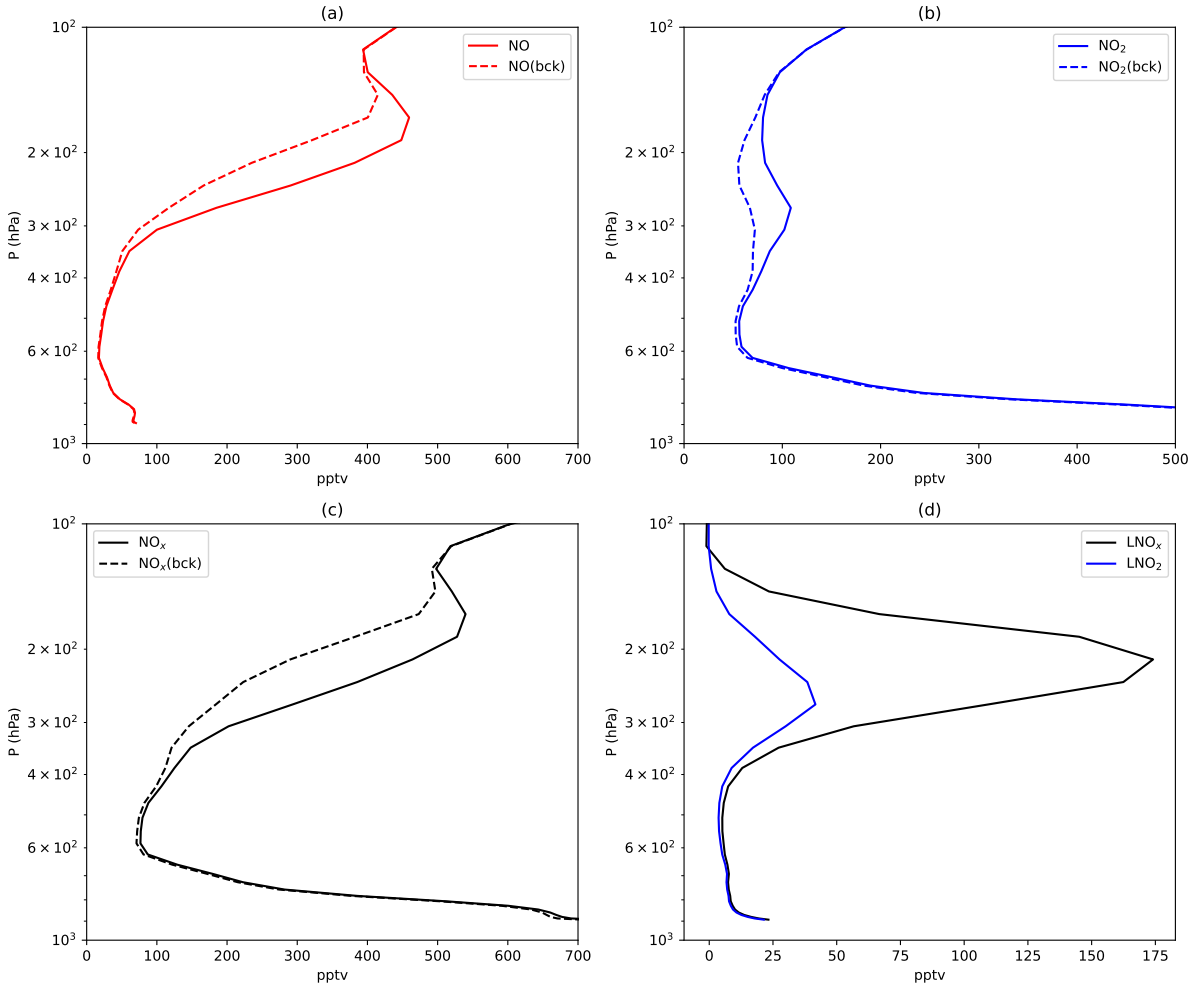

Figure S14. Vertical mixing ratio profiles of NO (a), NO_2 (b), NO_x (c), LNO_x and LNO_2 (d) extracted from WRF-CHEM simulations with (solid lines) and without (dashed lines) fresh LNO_x on 23 August 2024 at 12:10 UTC (close to the TROPOMI overpass (background: bck)).

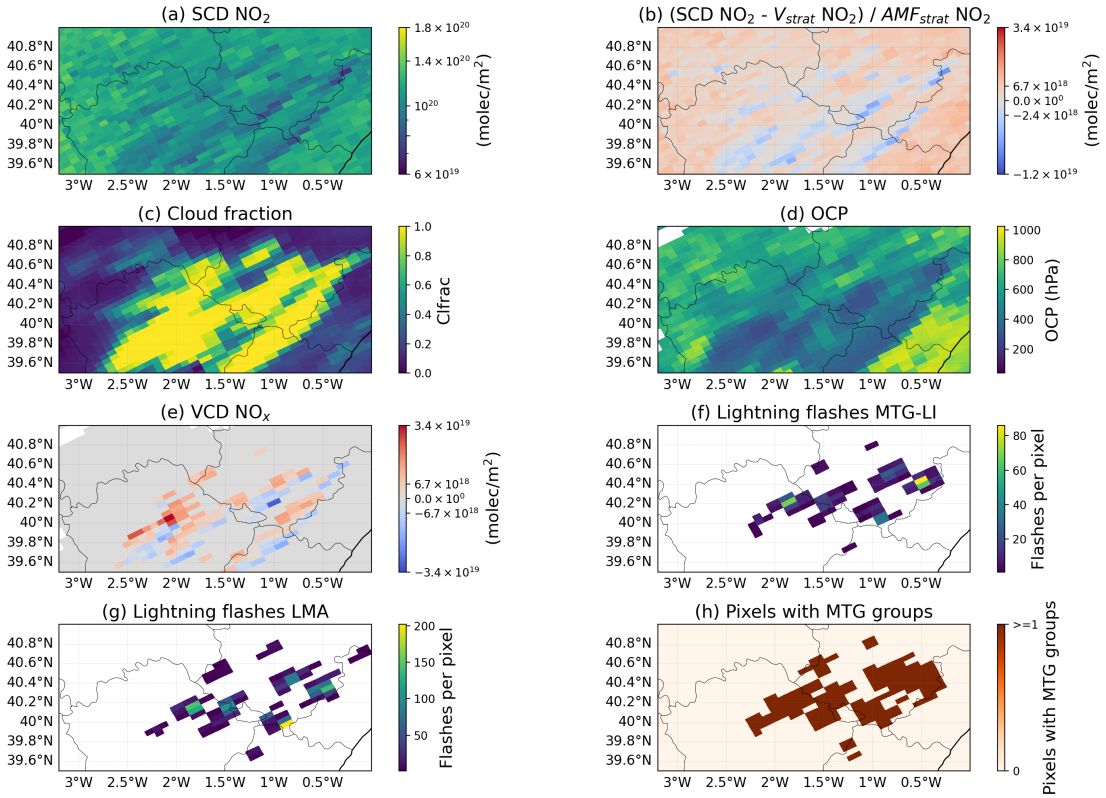

Figure S15. TROP-DLR product of orbit 35555, MTG-LI and LMA lightning data for the case 23 August 2024. (a): Slant Column Density (SCD) of NO_2 provided by the TROP-DLR NO_2 research product. (b): SCD NO_2 minus the stratospheric vertical column density and divided to the stratospheric air mass factor of NO_2 obtained from the TROP-DLR NO_2 research product. (c) and (d): Cloud Fraction (CF) and Optical Centroid Pressure (OCP) from the TROP-DLR NO_2 research product, respectively. (e): VCD of NO_x ($V_{tropNOx}$) over pixels satisfying the DCC. (f) and (g): Lightning flashes during the 5 h period per TROPOMI pixel before the TROPOMI overpass reported by MTG-LI and the LMA, respectively. (h): TROPOMI pixels containing at least one lightning group detected by MTG-LI.

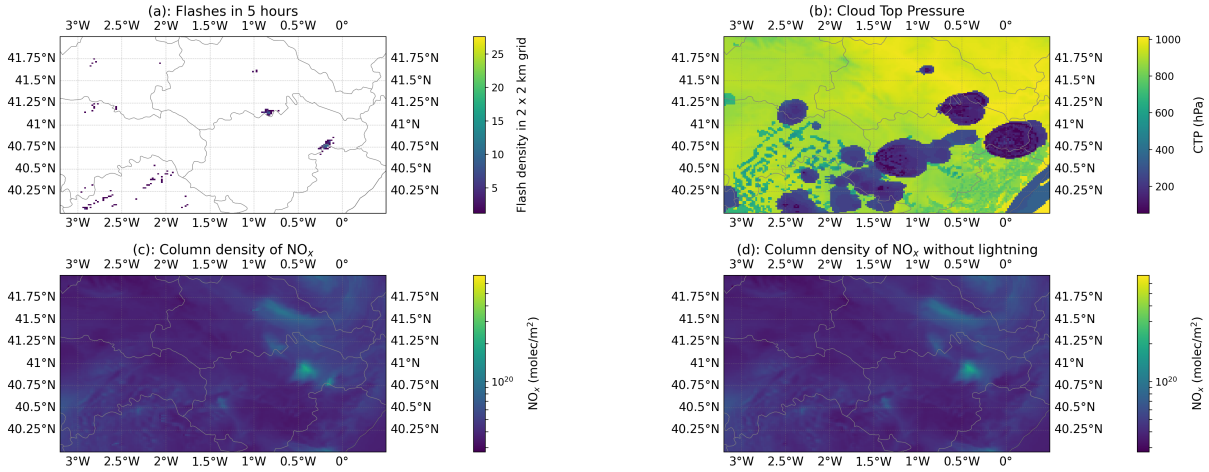

Figure S16. Simulation results for 25 August 2024 at 13:10 UTC, focused on the region of interest. (a): Assimilated lightning flashes between 08:10 and 13:10 UTC reported by MTG-LI. (b): Cloud Top Pressure (CTP). (c): Vertical Column Density of NO_x. (d): Vertical column density of NO_x in the simulation without fresh LNO_x, i.e., with LNO_x deactivated after 07:00 UTC.

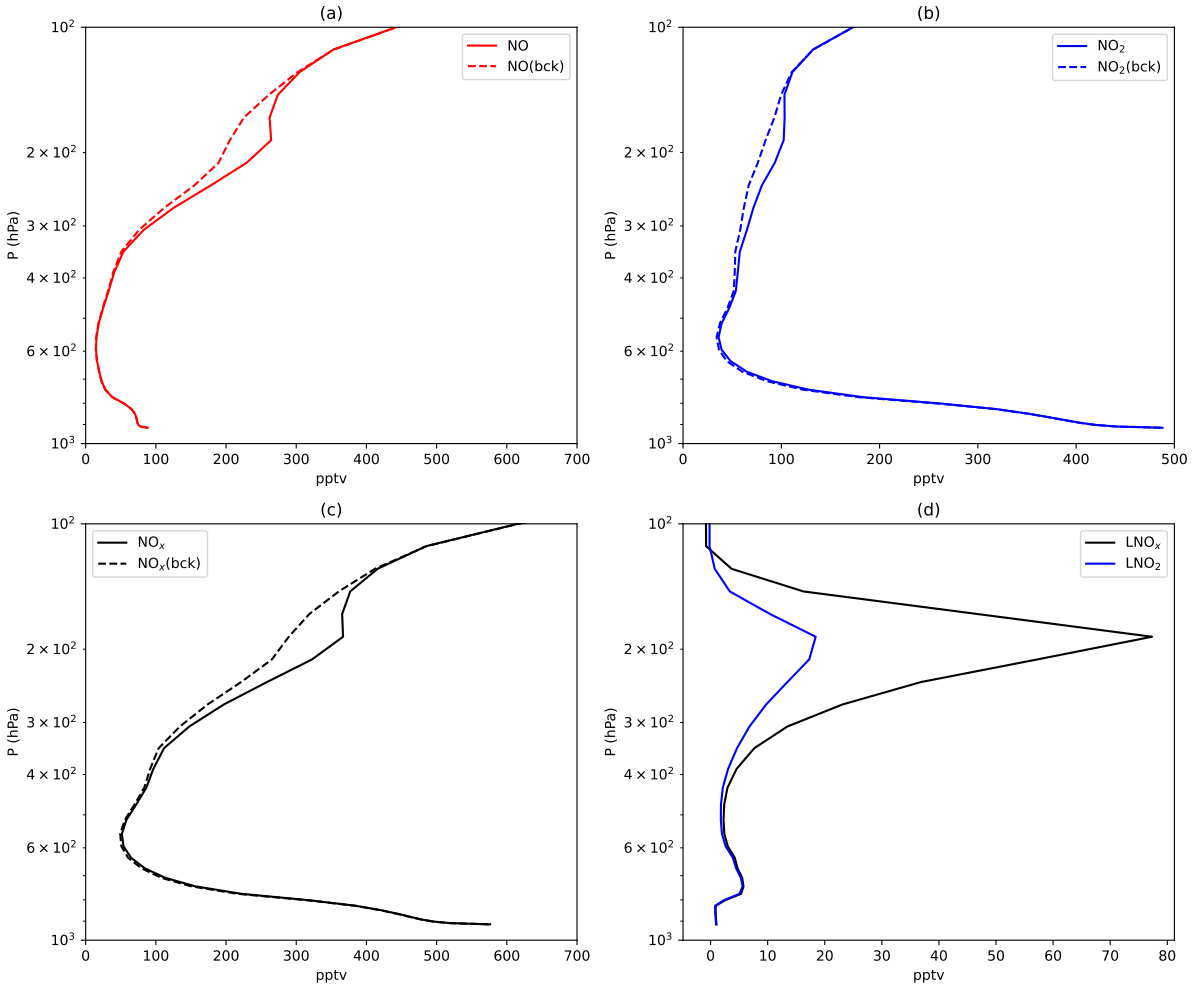

Figure S17. Vertical mixing ratio profiles of NO (a), NO_2 (b), NO_x (c), LNO_x and LNO_2 (d) extracted from WRF-CHEM simulations with (solid lines) and without (dashed lines) fresh LNO_x on 25 August 2024 at 13:10 UTC (close to the TROPOMI overpass (background: bck)).

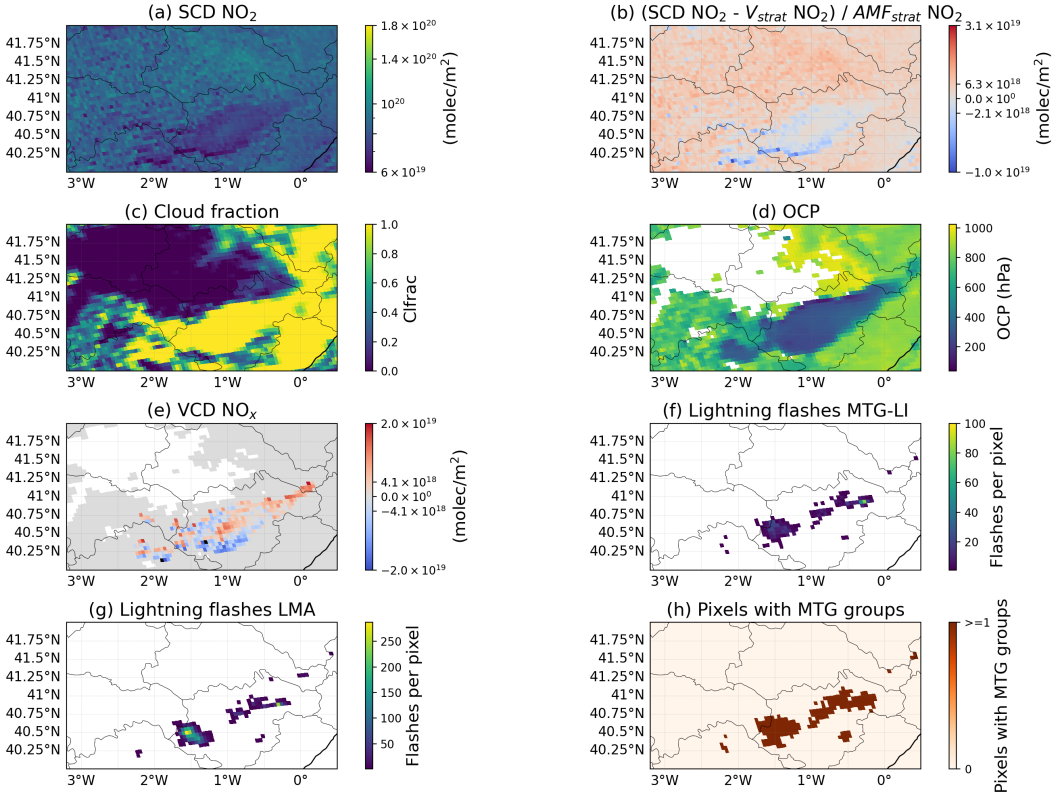

Figure S18. TROP-DLR product of orbit 35584, MTG-LI and LMA lightning data for the case 25 August 2024. (a): Slant Column Density (SCD) of NO_2 provided by the TROP-DLR NO_2 research product. (b): SCD NO_2 minus the stratospheric vertical column density and divided to the stratospheric air mass factor of NO_2 obtained from the TROP-DLR NO_2 research product. (c) and (d): Cloud Fraction (CF) and Optical Centroid Pressure (OCP) from the TROP-DLR NO_2 research product, respectively. (e): VCD of NO_x ($V_{tropNOx}$) over pixels satisfying the DCC. (f) and (g): Lightning flashes during the 5 h period per TROPOMI pixel before the TROPOMI overpass reported by MTG-LI and the LMA, respectively. (h): TROPOMI pixels containing at least one lightning group detected by MTG-LI.

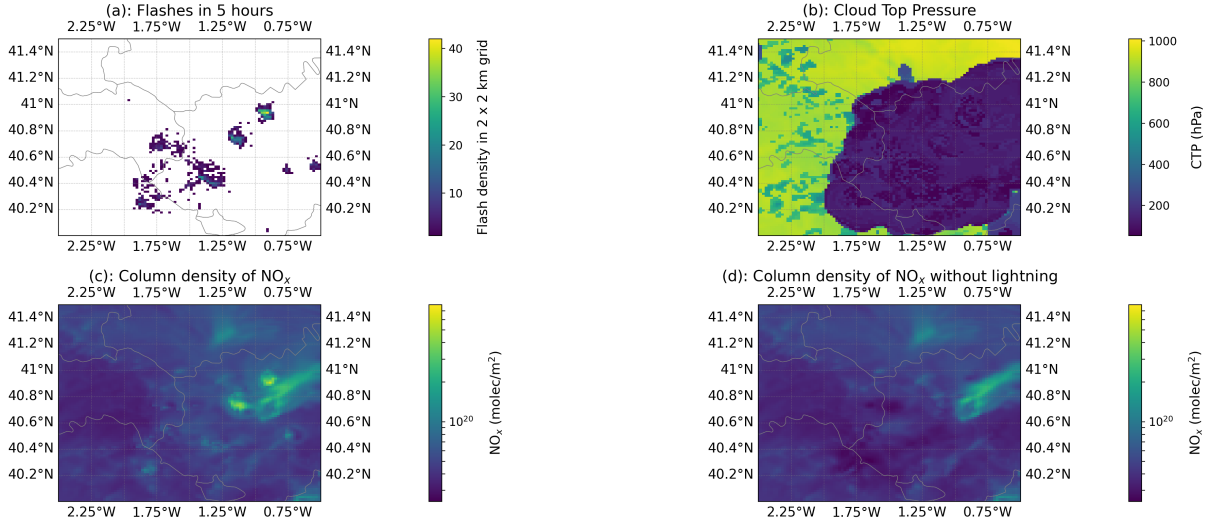

Figure S19. Simulation results for 2 September 2024 at 12:20 UTC, focused on the region of interest. (a): Assimilated lightning flashes between 07:20 and 12:20 UTC reported by MTG-LI. (b): Cloud Top Pressure (CTP). (c): Vertical Column Density of NO_x. (d): Vertical column density of NO_x in the simulation without fresh LNO_x, i.e., with LNO_x deactivated after 07:00 UTC.

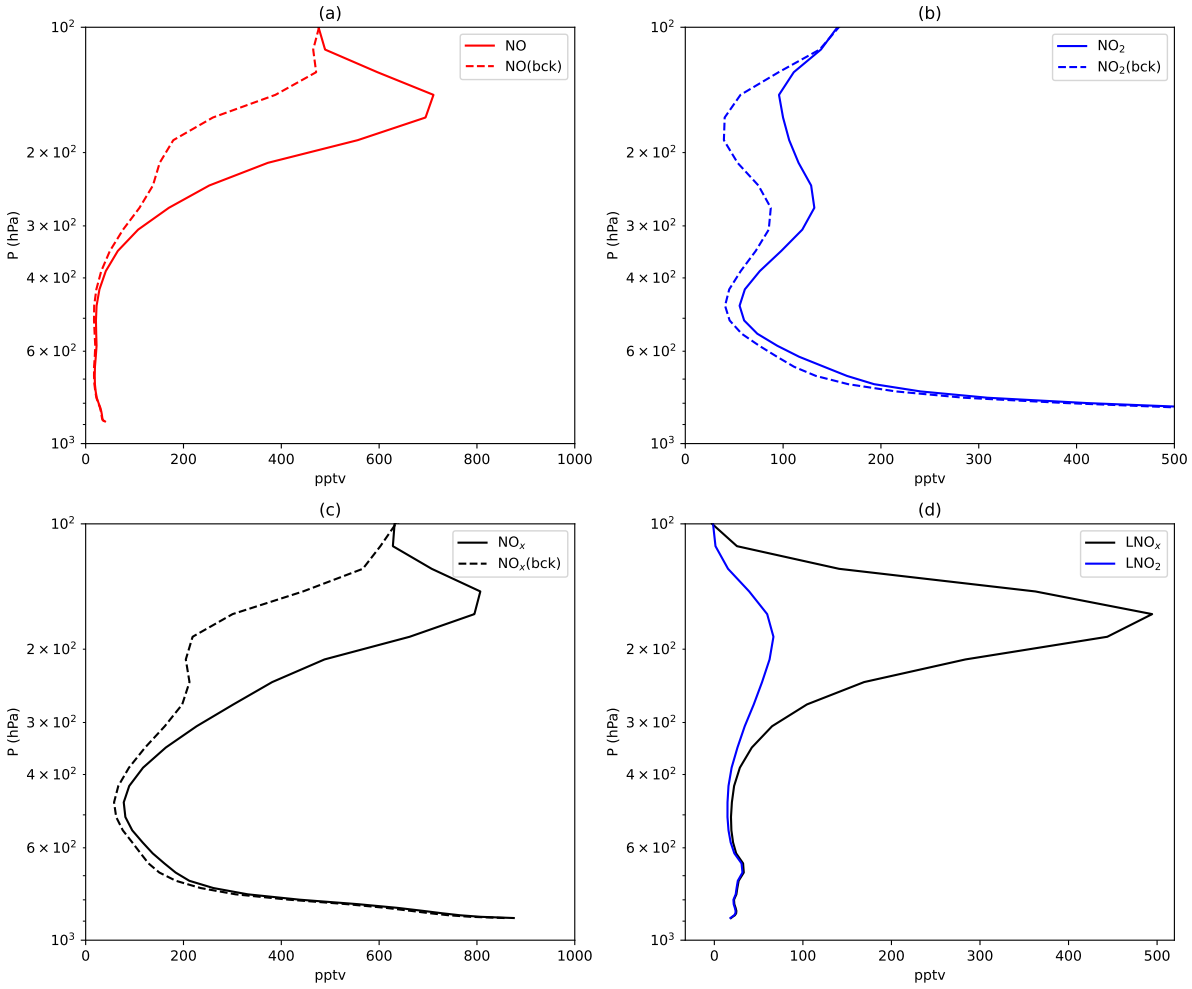

Figure S20. Vertical mixing ratio profiles of NO (a), NO_2 (b), NO_x (c), LNO_x and LNO_2 (d) extracted from WRF-CHEM simulations with (solid lines) and without (dashed lines) fresh LNO_x on 2 September 2024 at 12:20 UTC (close to the TROPOMI overpass (background: bck)).

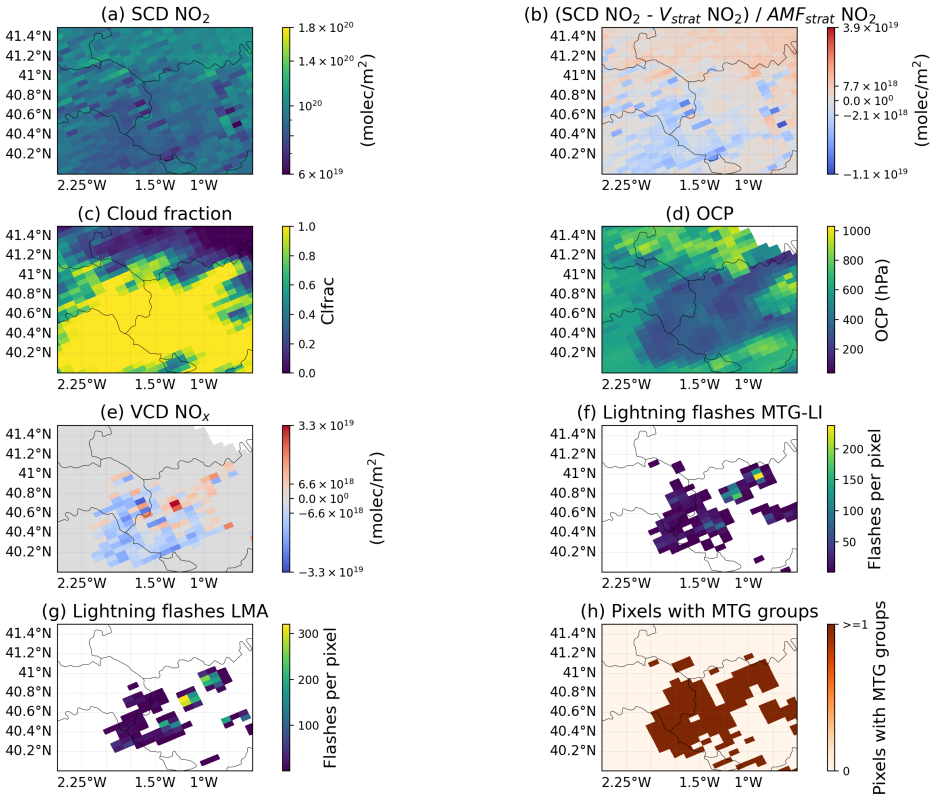

Figure S21. TROP-DLR product of orbit 35697, MTG-LI and LMA lightning data for the case 2 September 2024. (a): Slant Column Density (SCD) of NO_2 provided by the TROP-DLR NO_2 research product. (b): SCD NO_2 minus the stratospheric vertical column density and divided to the stratospheric air mass factor of NO_2 obtained from the TROP-DLR NO_2 research product. (c) and (d): Cloud Fraction (CF) and Optical Centroid Pressure (OCP) from the TROP-DLR NO_2 research product, respectively. (e): VCD of NO_x ($V_{tropNOx}$) over pixels satisfying the DCC. (f) and (g): Lightning flashes during the 5 h period per TROPOMI pixel before the TROPOMI overpass reported by MTG-LI and the LMA, respectively. (h): TROPOMI pixels containing at least one lightning group detected by MTG-LI.

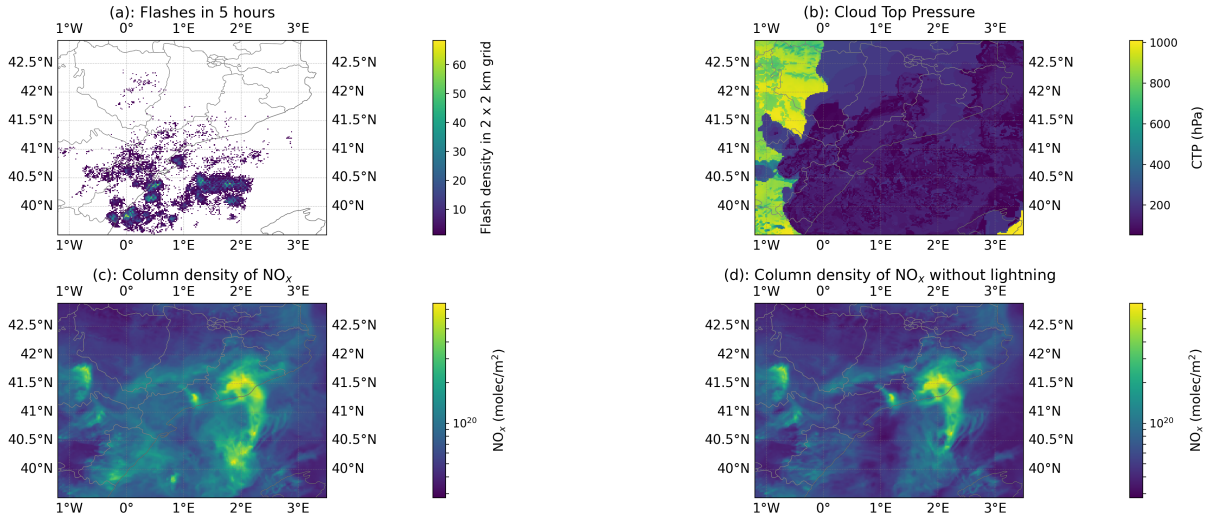

Figure S22. Simulation results for 3 September 2024 at 12:00 UTC, focused on the region of interest. (a): Assimilated lightning flashes between 07:00 and 12:00 UTC reported by MTG-LI. (b): Cloud Top Pressure (CTP). (c): Vertical Column Density of NO_x. (d): Vertical column density of NO_x in the simulation without fresh LNO_x, i.e., with LNO_x deactivated after 07:00 UTC.

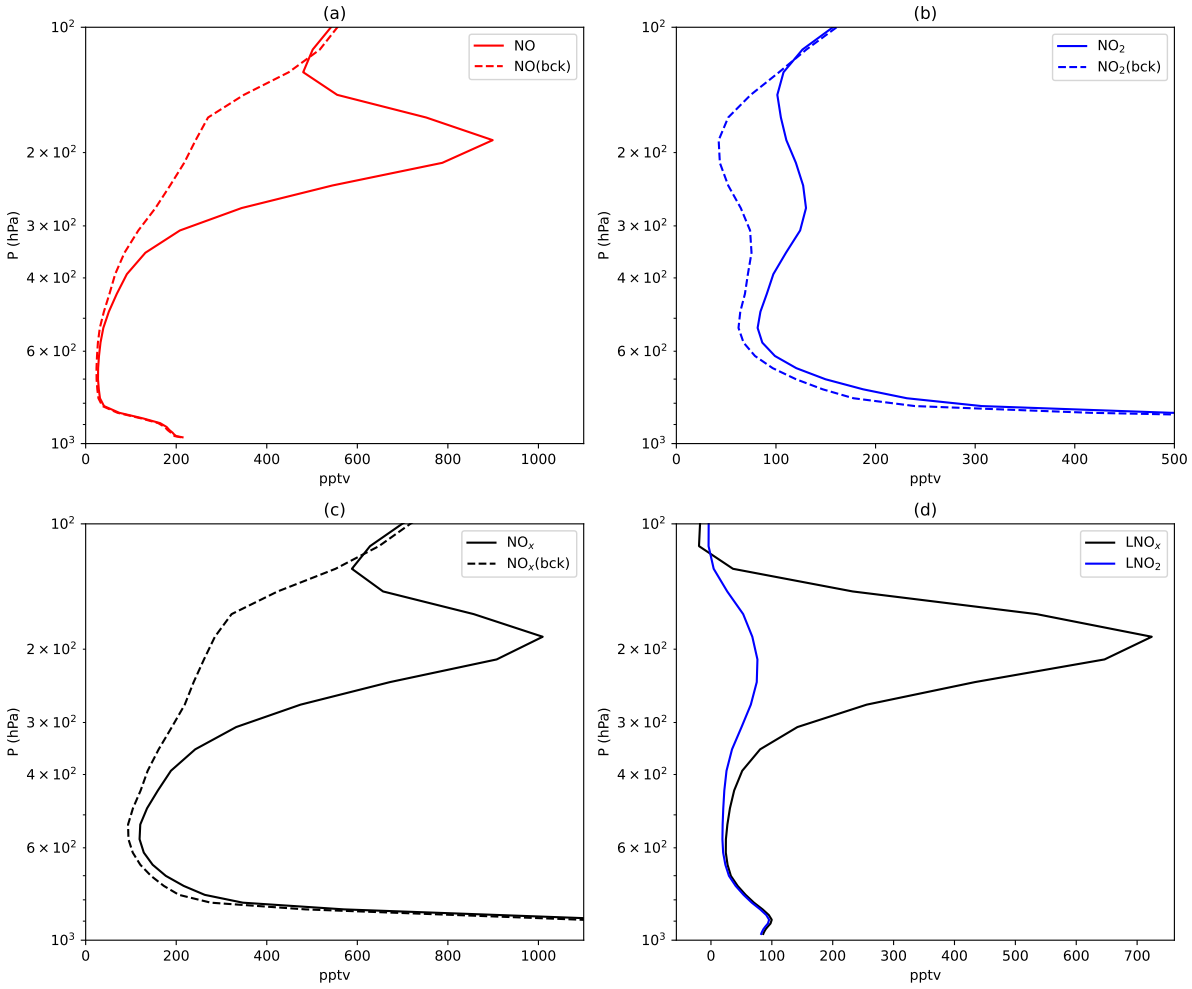

Figure S23. Vertical mixing ratio profiles of NO (a), NO_2 (b), NO_x (c), LNO_x and LNO_2 (d) extracted from WRF-CHEM simulations with (solid lines) and without (dashed lines) fresh LNO_x on 3 September 2024 at 12:00 UTC (close to the TROPOMI overpass (background: bck)).

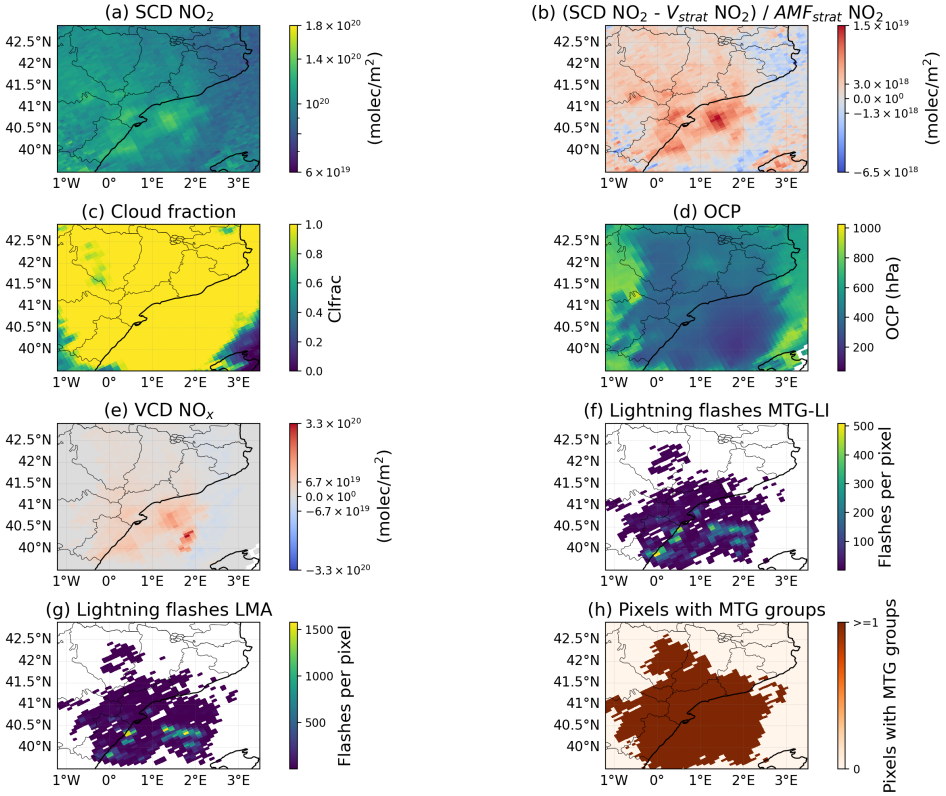

Figure S24. TROP-DLR product of orbit 35711, MTG-LI and LMA lightning data for the case 3 September 2024. (a): Slant Column Density (SCD) of NO_2 provided by the TROP-DLR NO_2 research product. (b): SCD NO_2 minus the stratospheric vertical column density and divided to the stratospheric air mass factor of NO_2 obtained from the TROP-DLR NO_2 research product. (c) and (d): Cloud Fraction (CF) and Optical Centroid Pressure (OCP) from the TROP-DLR NO_2 research product, respectively. (e): VCD of NO_x ($V_{tropNOx}$) over pixels satisfying the DCC. (f) and (g): Lightning flashes during the 5 h period per TROPOMI pixel before the TROPOMI overpass reported by MTG-LI and the LMA, respectively. (h): TROPOMI pixels containing at least one lightning group detected by MTG-LI.

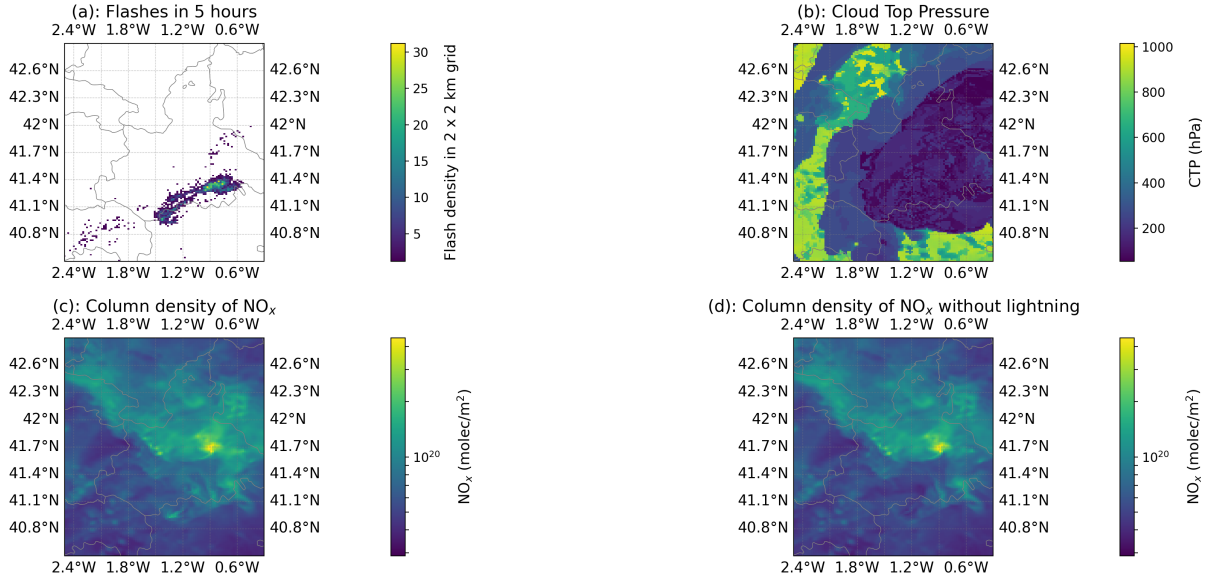

Figure S25. Simulation results for 21 September 2024 at 13:10 UTC, focused on the region of interest. (a): Assimilated lightning flashes between 08:10 and 13:10 UTC reported by MTG-LI. (b): Cloud Top Pressure (CTP). (c): Vertical Column Density of NO_x. (d): Vertical column density of NO_x in the simulation without fresh LNO_x, i.e., with LNO_x deactivated after 07:00 UTC.

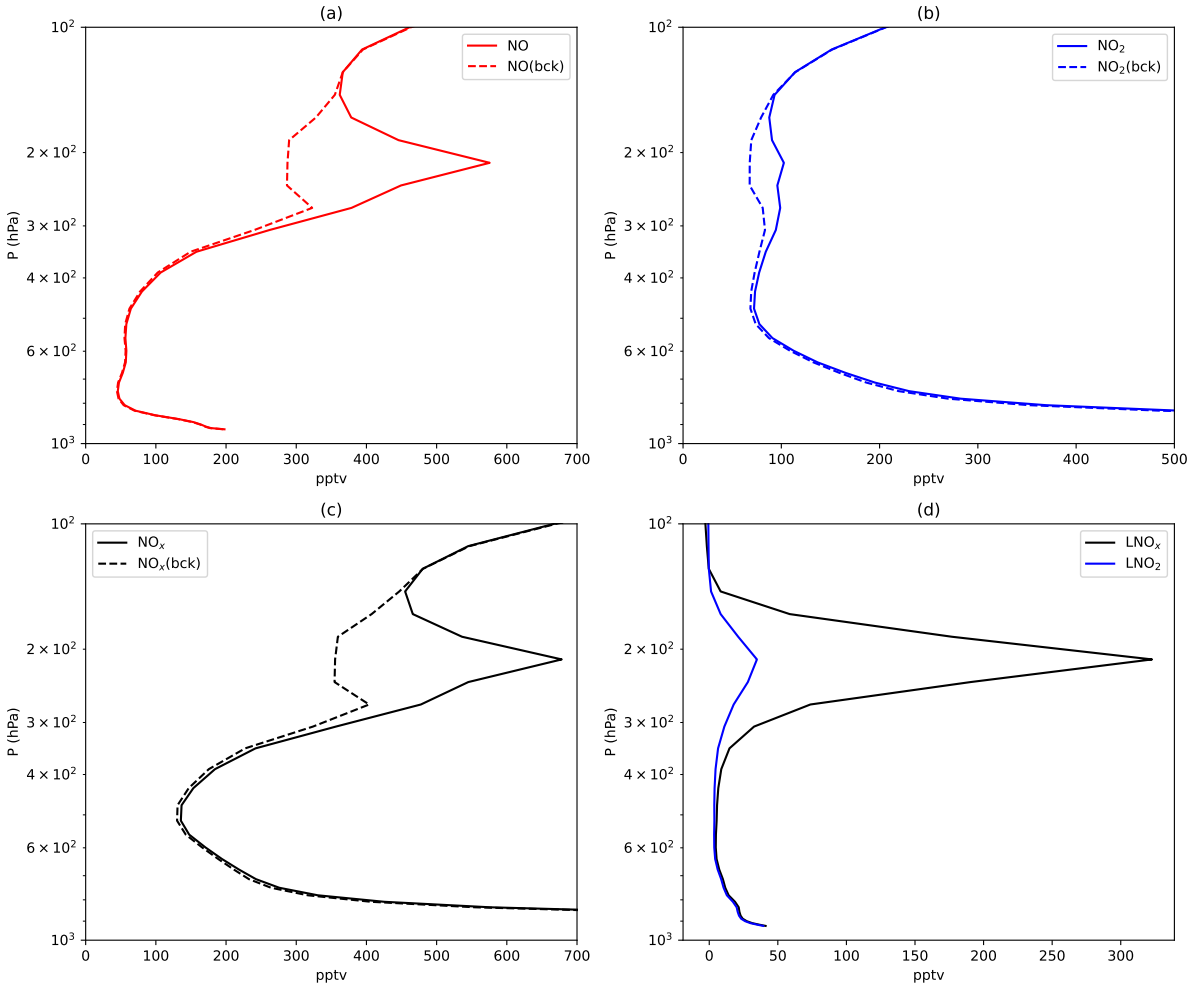

Figure S26. Vertical mixing ratio profiles of NO (a), NO_2 (b), NO_x (c), LNO_x and LNO_2 (d) extracted from WRF-CHEM simulations with (solid lines) and without (dashed lines) fresh LNO_x on 21 September 2024 at 13:10 UTC (close to the TROPOMI overpass (background: bck)).

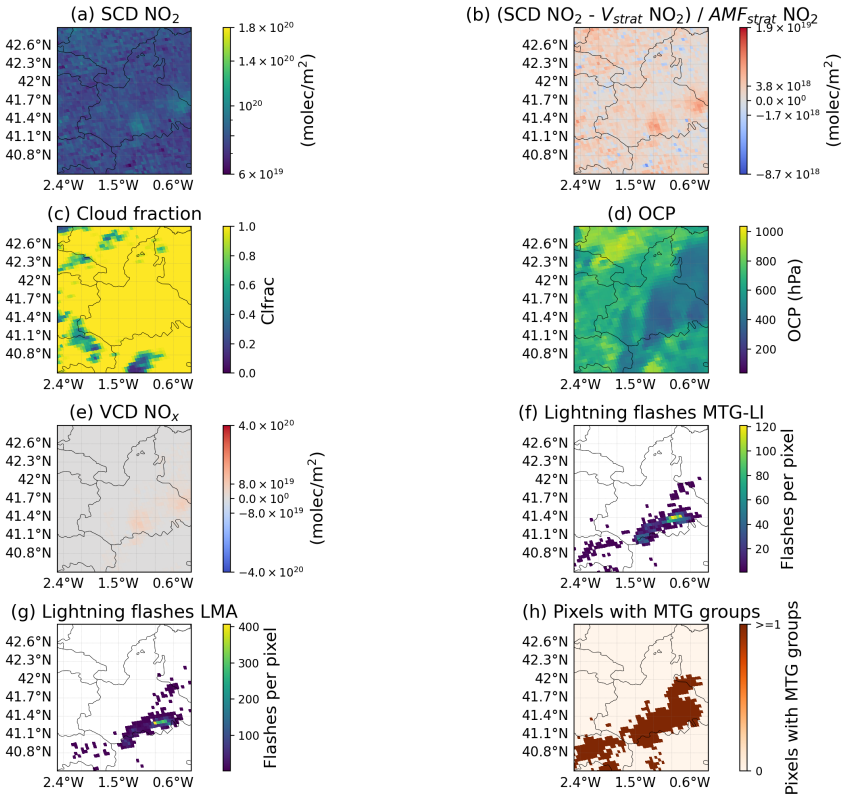

Figure S27. TROP-DLR product of orbit 35967, MTG-LI and LMA lightning data for the case 21 September 2024. (a): Slant Column Density (SCD) of NO_2 provided by the TROP-DLR NO_2 research product. (b): SCD NO_2 minus the stratospheric vertical column density and divided to the stratospheric air mass factor of NO_2 obtained from the TROP-DLR NO_2 research product. (c) and (d): Cloud Fraction (CF) and Optical Centroid Pressure (OCP) from the TROP-DLR NO_2 research product, respectively. (e): VCD of NO_x ($V_{tropNOx}$) over pixels satisfying the DCC. (f) and (g): Lightning flashes during the 5 h period per TROPOMI pixel before the TROPOMI overpass reported by MTG-LI and the LMA, respectively. (h): TROPOMI pixels containing at least one lightning group detected by MTG-LI.

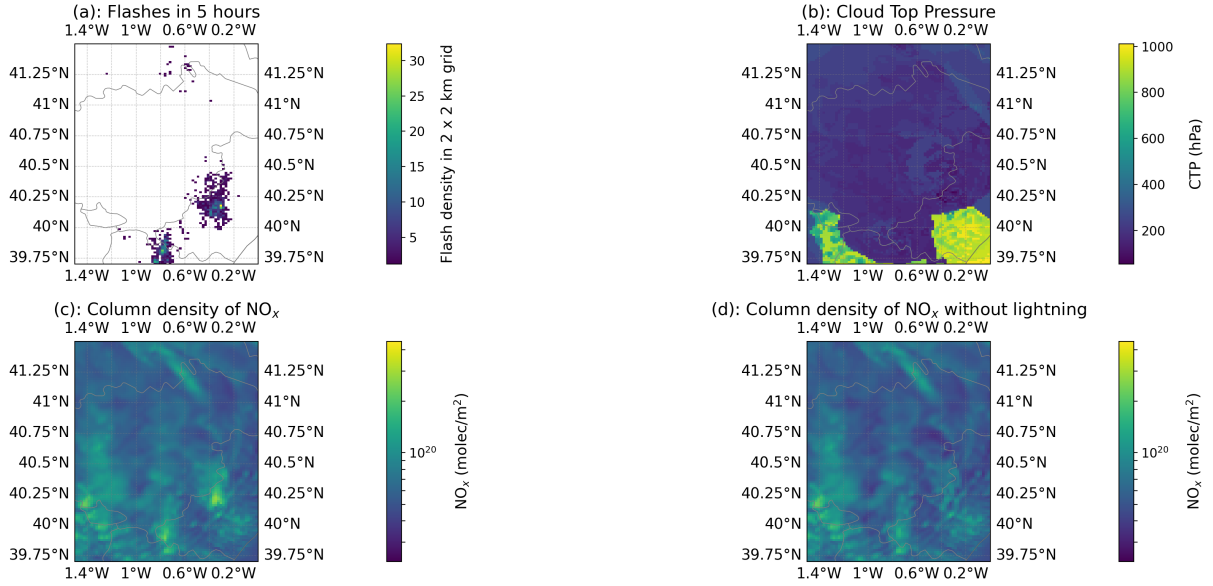

Figure S28. Simulation results for 15 October 2024 at 12:10 UTC, focused on the region of interest. (a): Assimilated lightning flashes between 07:10 and 12:10 UTC reported by MTG-LI. (b): Cloud Top Pressure (CTP). (c): Vertical Column Density of NO_x. (d): Vertical column density of NO_x in the simulation without fresh LNO_x, i.e., with LNO_x deactivated after 07:00 UTC.

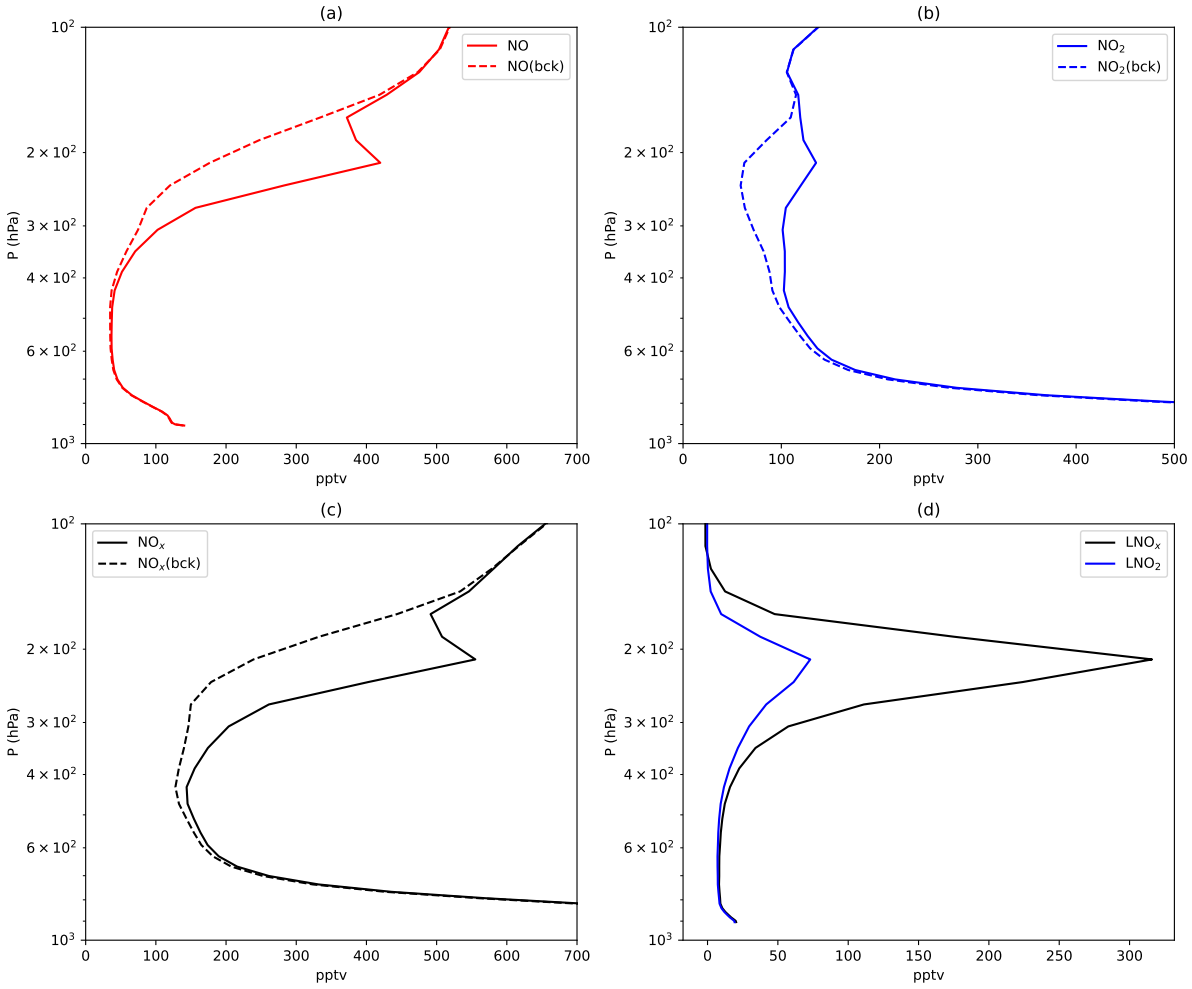

Figure S29. Vertical mixing ratio profiles of NO (a), NO_2 (b), NO_x (c), LNO_x and LNO_2 (d) extracted from WRF-CHEM simulations with (solid lines) and without (dashed lines) fresh LNO_x on 15 October 2024 at 12:10 UTC (close to the TROPOMI overpass (background: bck)).

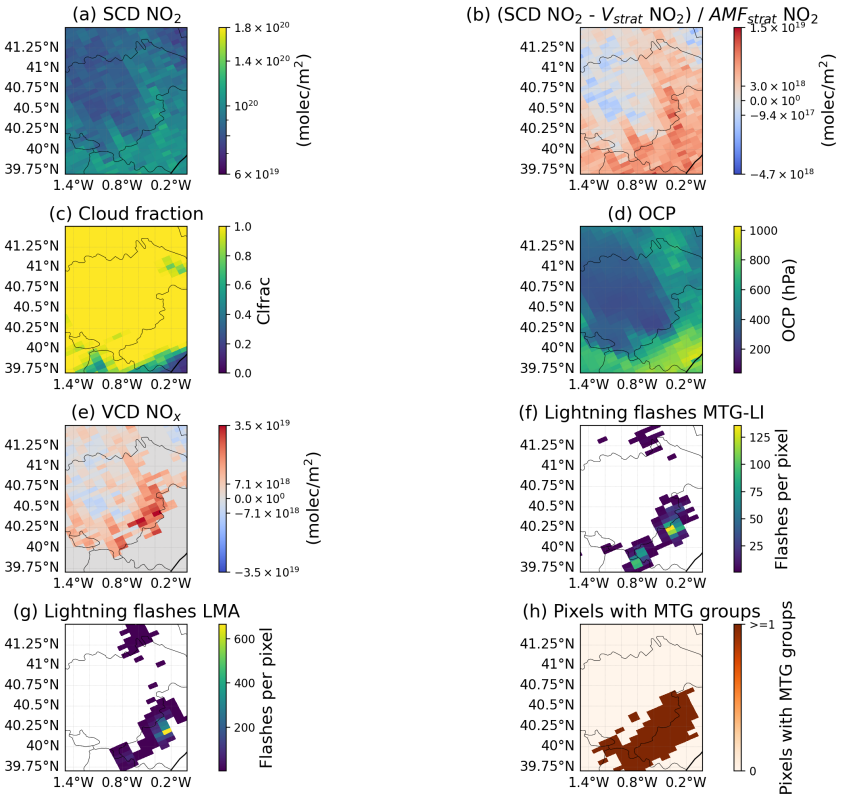

Figure S30. TROP-DLR product of orbit 36307, MTG-LI and LMA lightning data for the case 15 October 2024. (a): Slant Column Density (SCD) of NO_2 provided by the TROP-DLR NO_2 research product. (b): SCD NO_2 minus the stratospheric vertical column density and divided to the stratospheric air mass factor of NO_2 obtained from the TROP-DLR NO_2 research product. (c) and (d): Cloud Fraction (CF) and Optical Centroid Pressure (OCP) from the TROP-DLR NO_2 research product, respectively. (e): VCD of NO_x ($V_{tropNOx}$) over pixels satisfying the DCC. (f) and (g): Lightning flashes during the 5 h period per TROPOMI pixel before the TROPOMI overpass reported by MTG-LI and the LMA, respectively. (h): TROPOMI pixels containing at least one lightning group detected by MTG-LI.

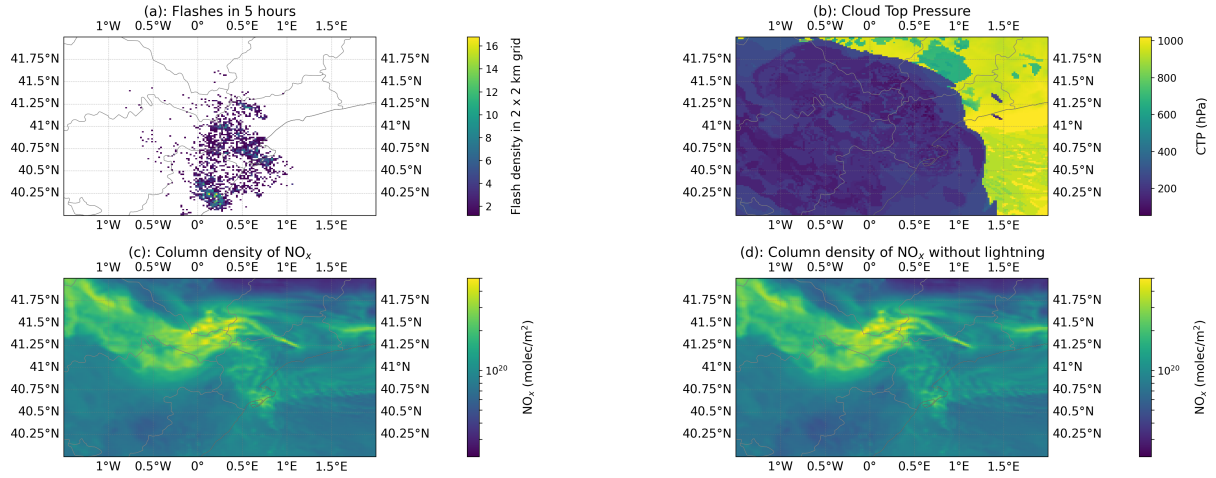

Figure S31. Simulation results for 31 October 2024 at 12:30 UTC, focused on the region of interest. (a): Assimilated lightning flashes between 07:30 and 12:30 UTC reported by MTG-LI. (b): Cloud Top Pressure (CTP). (c): Vertical Column Density of NO_x. (d): Vertical column density of NO_x in the simulation without fresh LNO_x, i.e., with LNO_x deactivated after 07:00 UTC.

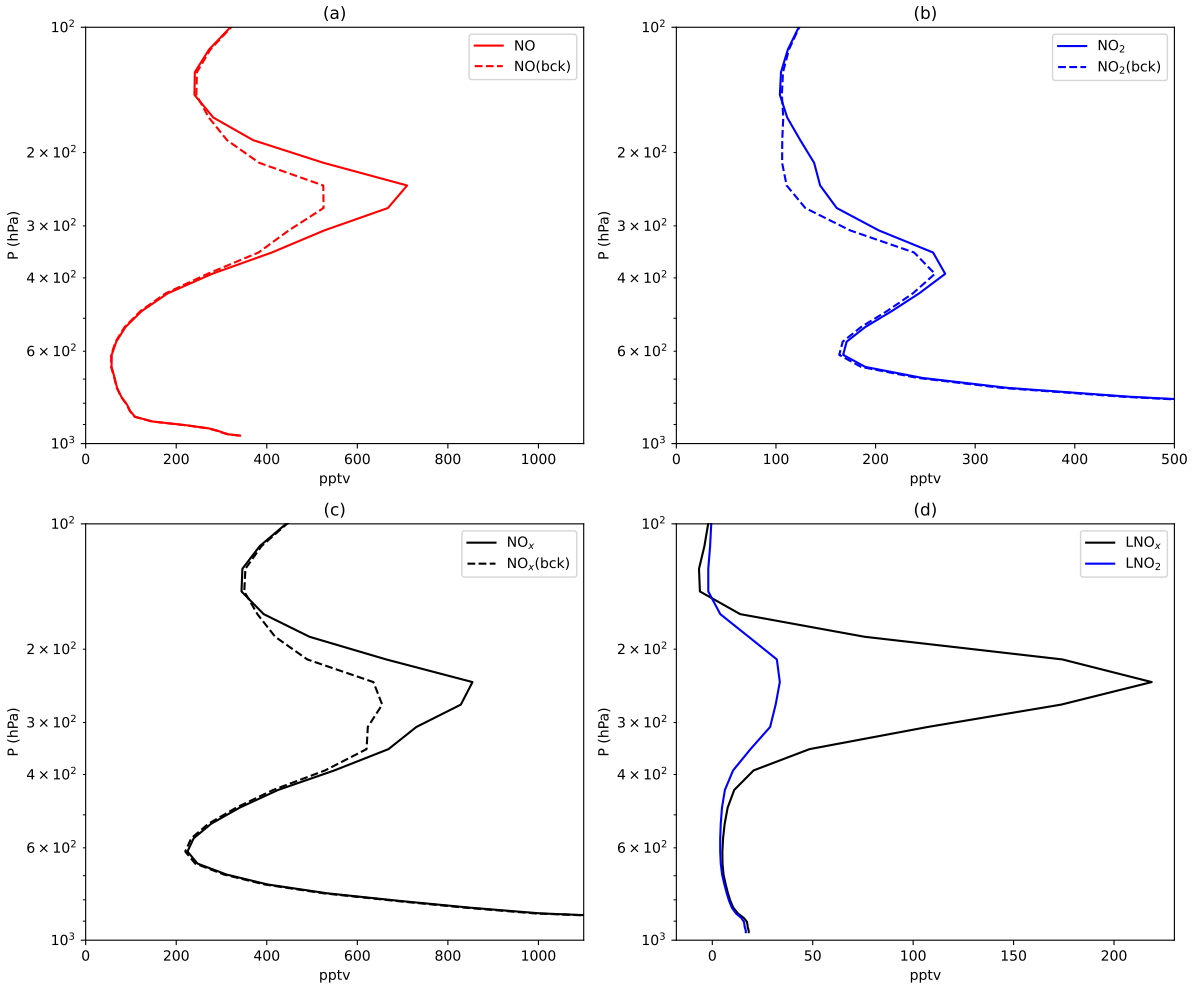

Figure S32. Vertical mixing ratio profiles of NO (a), NO_2 (b), NO_x (c), LNO_x and LNO_2 (d) extracted from WRF-CHEM simulations with (solid lines) and without (dashed lines) fresh LNO_x on 31 October 2024 at 12:30 UTC (close to the TROPOMI overpass (background: bck)).

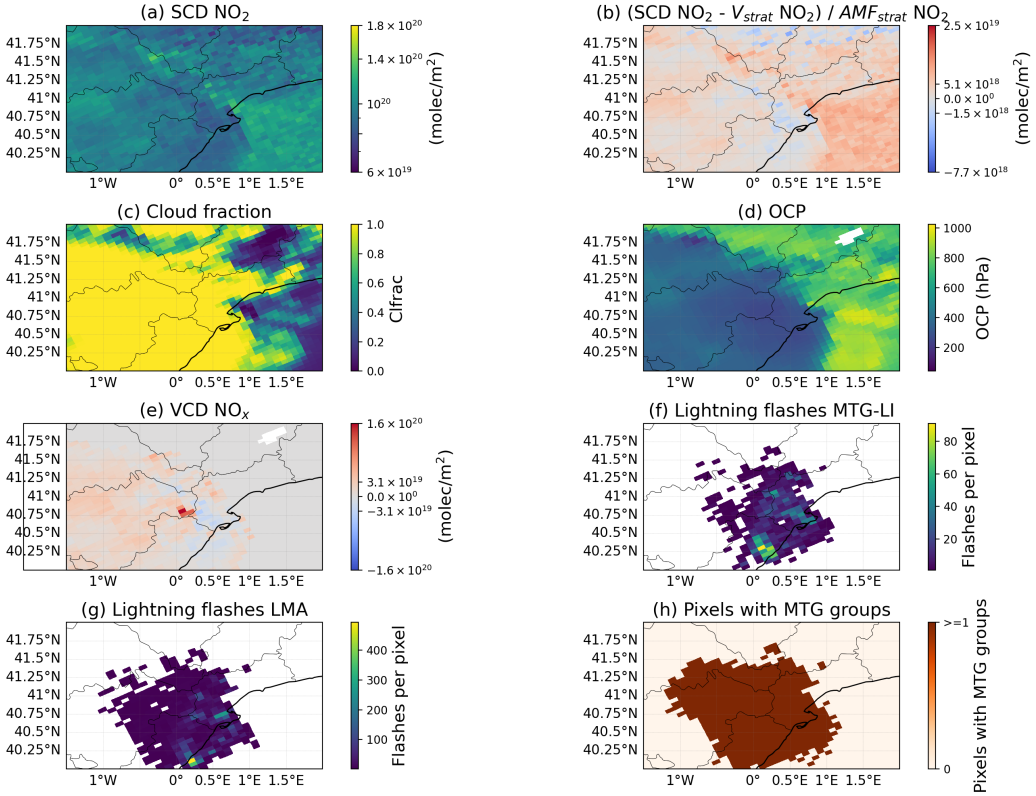

Figure S33. TROP-DLR product of orbit 36534, MTG-LI and LMA lightning data for the case 31 October 2024. (a): Slant Column Density (SCD) of NO_2 provided by the TROP-DLR NO_2 research product. (b): SCD NO_2 minus the stratospheric vertical column density and divided to the stratospheric air mass factor of NO_2 obtained from the TROP-DLR NO_2 research product. (c) and (d): Cloud Fraction (CF) and Optical Centroid Pressure (OCP) from the TROP-DLR NO_2 research product, respectively. (e): VCD of NO_x ($V_{tropNOx}$) over pixels satisfying the DCC. (f) and (g): Lightning flashes during the 5 h period per TROPOMI pixel before the TROPOMI overpass reported by MTG-LI and the LMA, respectively. (h): TROPOMI pixels containing at least one lightning group detected by MTG-LI.

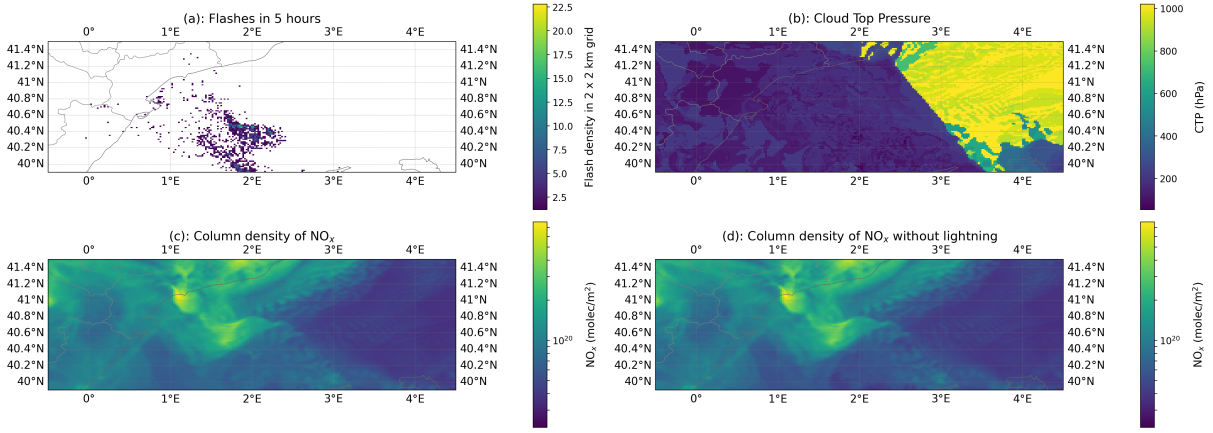

Figure S34. Simulation results for 1 November 2024 at 13:40 UTC, focused on the region of interest. (a): Assimilated lightning flashes between 08:40 and 13:40 UTC reported by MTG-LI. (b): Cloud Top Pressure (CTP). (c): Vertical Column Density of NO_x. (d): Vertical column density of NO_x in the simulation without fresh LNO_x, i.e., with LNO_x deactivated after 07:00 UTC.

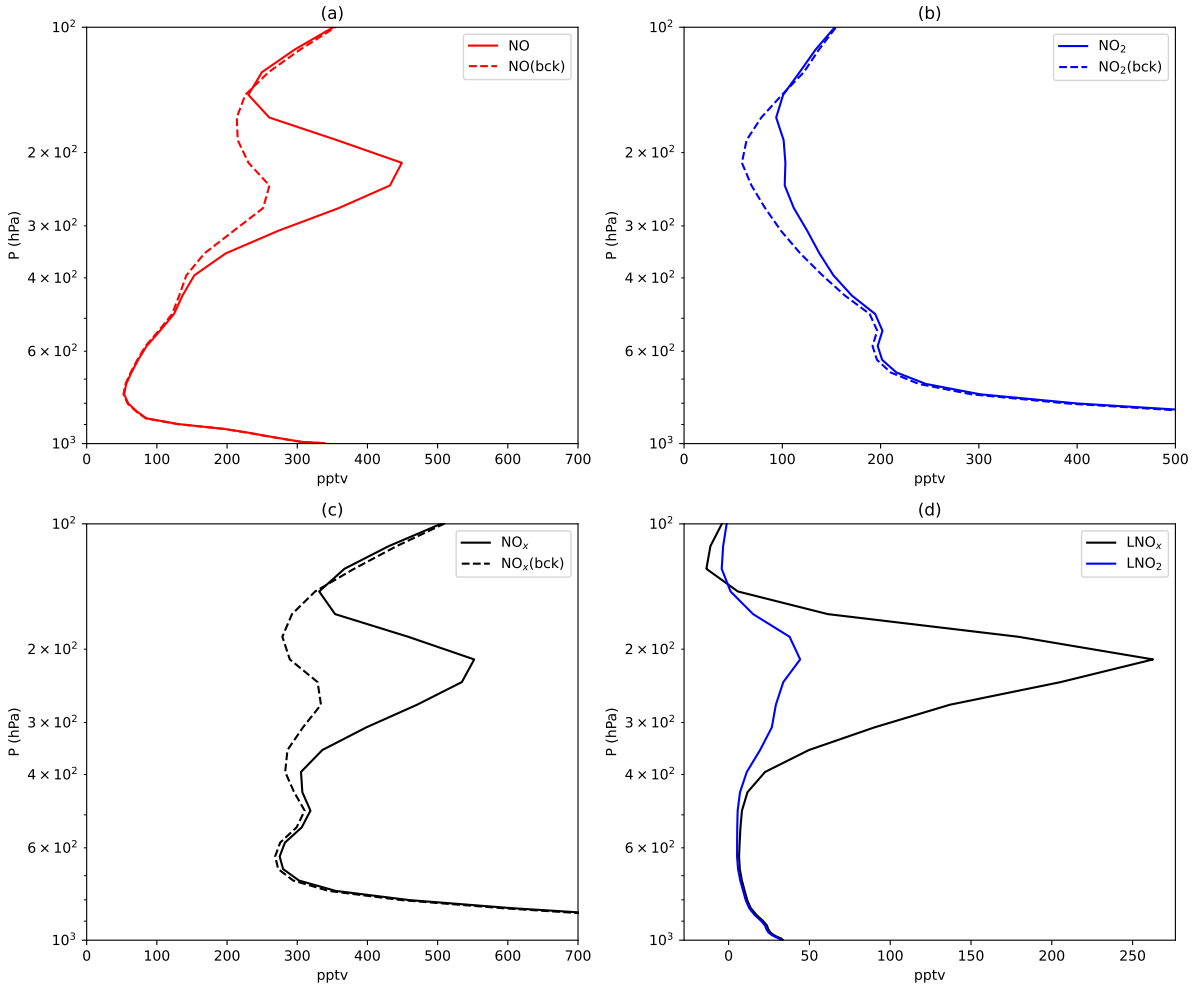

Figure S35. Vertical mixing ratio profiles of NO (a), NO_2 (b), NO_x (c), LNO_x and LNO_2 (d) extracted from WRF-CHEM simulations with (solid lines) and without (dashed lines) fresh LNO_x on 1 November 2024 at 13:40 UTC (close to the TROPOMI overpass (background: bck)).

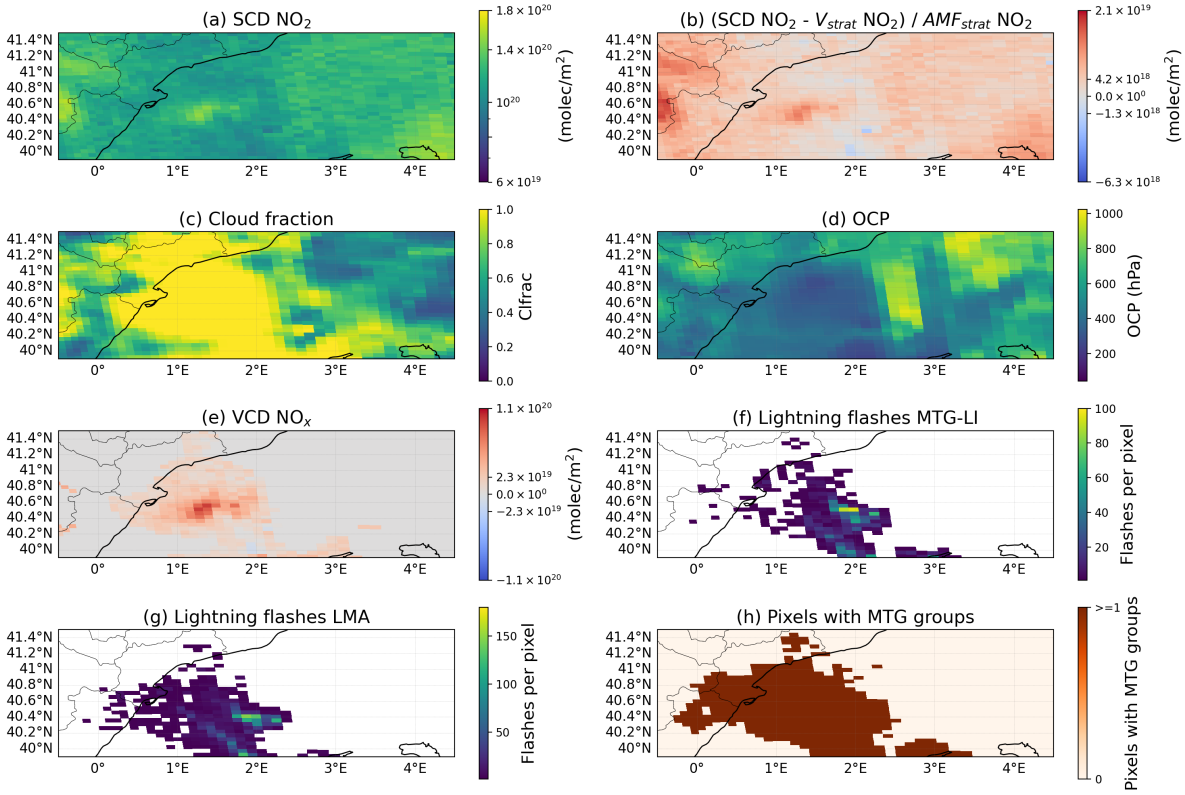

Figure S36. TROP-DLR product of orbit 36549, MTG-LI and LMA lightning data for the case 1 November 2024. (a): Slant Column Density (SCD) of NO_2 provided by the TROP-DLR NO_2 research product. (b): SCD NO_2 minus the stratospheric vertical column density and divided to the stratospheric air mass factor of NO_2 obtained from the TROP-DLR NO_2 research product. (c) and (d): Cloud Fraction (CF) and Optical Centroid Pressure (OCP) from the TROP-DLR NO_2 research product, respectively. (e): VCD of NO_x ($V_{tropNOx}$) over pixels satisfying the DCC. (f) and (g): Lightning flashes during the 5 h period per TROPOMI pixel before the TROPOMI overpass reported by MTG-LI and the LMA, respectively. (h): TROPOMI pixels containing at least one lightning group detected by MTG-LI.

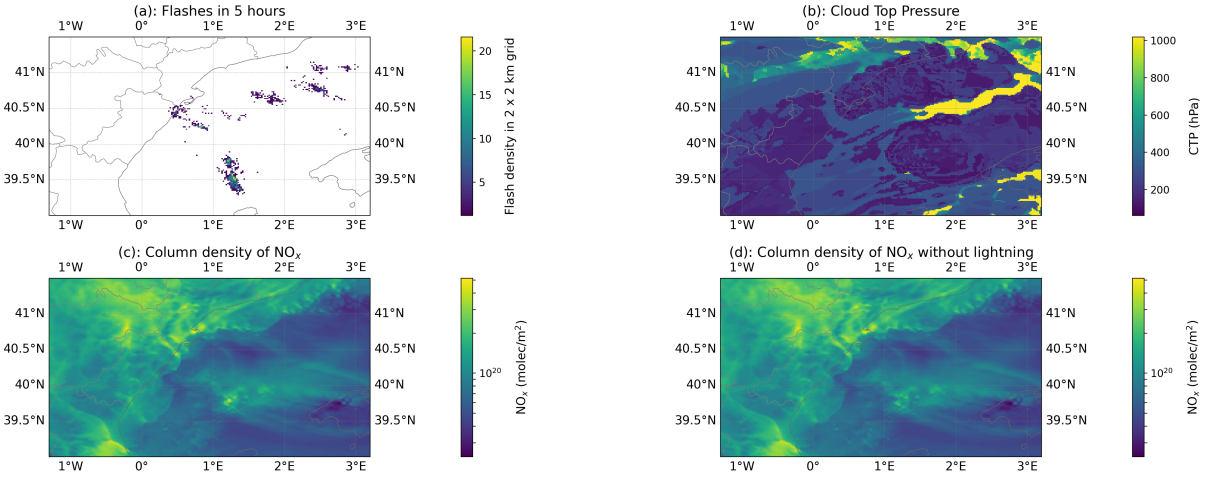

Figure S37. Simulation results for 13 November 2024 at 13:10 UTC, focused on the region of interest. (a): Assimilated lightning flashes between 08:10 and 13:10 UTC reported by MTG-LI. (b): Cloud Top Pressure (CTP). (c): Vertical Column Density of NO_x. (d): Vertical column density of NO_x in the simulation without fresh LNO_x, i.e., with LNO_x deactivated after 07:00 UTC.

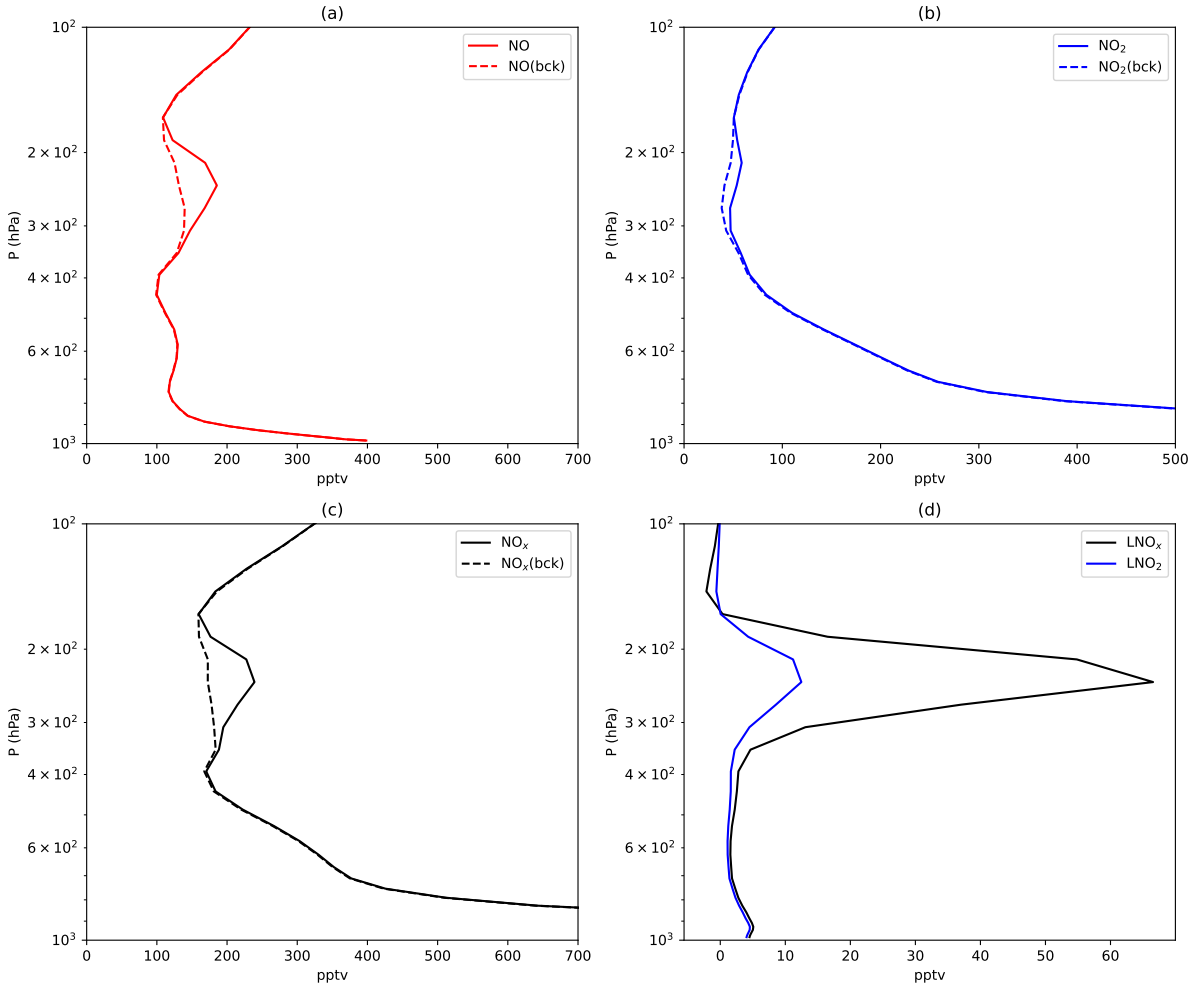

Figure S38. Vertical mixing ratio profiles of NO (a), NO_2 (b), NO_x (c), LNO_x and LNO_2 (d) extracted from WRF-CHEM simulations with (solid lines) and without (dashed lines) fresh LNO_x on 13 November 2024 at 13:10 UTC (close to the TROPOMI overpass (background: bck)).

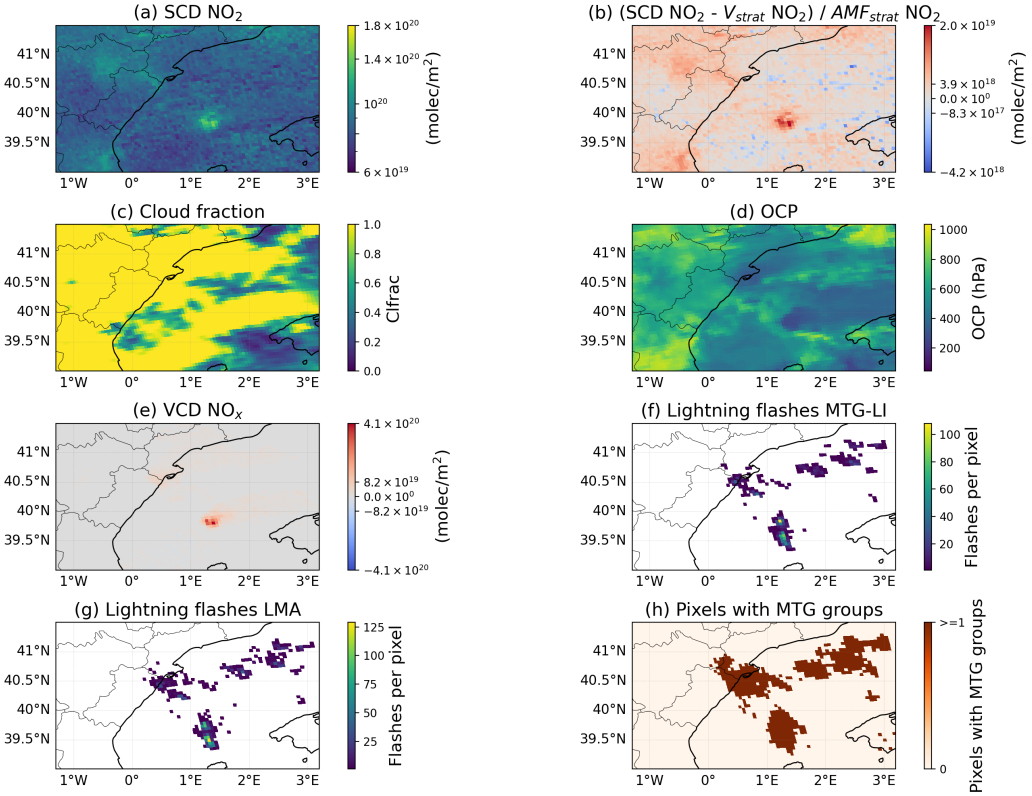

Figure S39. TROP-DLR product of orbit 36719, MTG-LI and LMA lightning data for the case 13 November 2024. (a): Slant Column Density (SCD) of NO_2 provided by the TROP-DLR NO_2 research product. (b): SCD NO_2 minus the stratospheric vertical column density and divided to the stratospheric air mass factor of NO_2 obtained from the TROP-DLR NO_2 research product. (c) and (d): Cloud Fraction (CF) and Optical Centroid Pressure (OCP) from the TROP-DLR NO_2 research product, respectively. (e): VCD of NO_x ($V_{tropNOx}$) over pixels satisfying the DCC. (f) and (g): Lightning flashes during the 5 h period per TROPOMI pixel before the TROPOMI overpass reported by MTG-LI and the LMA, respectively. (h): TROPOMI pixels containing at least one lightning group detected by MTG-LI.

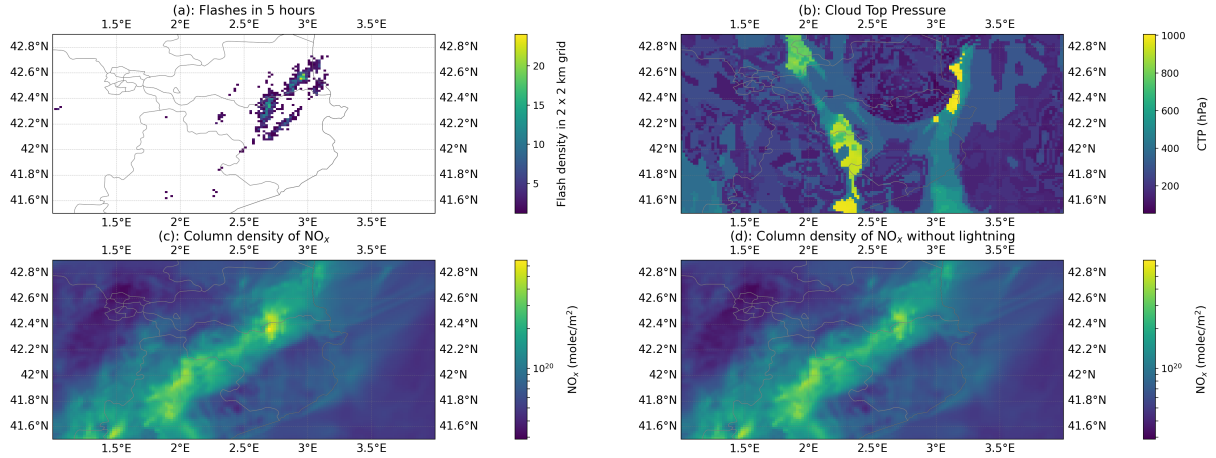

Figure S40. Simulation results for 15 April 2025 at 13:50 UTC, focused on the region of interest. (a): Assimilated lightning flashes between 08:50 and 13:50 UTC reported by MTG-LI. (b): Cloud Top Pressure (CTP). (c): Vertical Column Density of NO_x. (d): Vertical column density of NO_x in the simulation without fresh LNO_x, i.e., with LNO_x deactivated after 07:00 UTC.

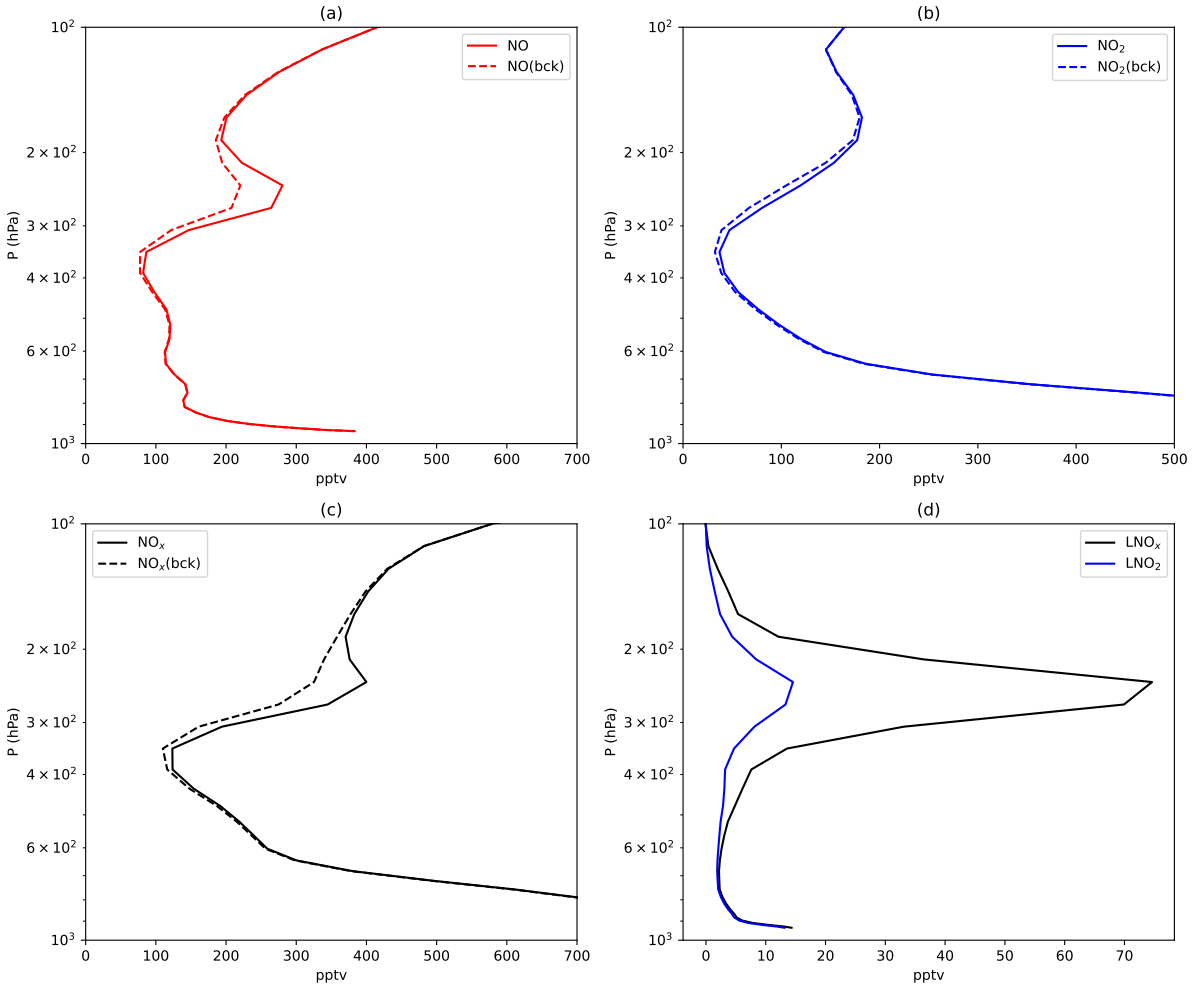

Figure S41. Vertical mixing ratio profiles of NO (a), NO_2 (b), NO_x (c), LNO_x and LNO_2 (d) extracted from WRF-CHEM simulations with (solid lines) and without (dashed lines) fresh LNO_x on 15 April 2025 at 13:50 UTC (close to the TROPOMI overpass (background: bck)).

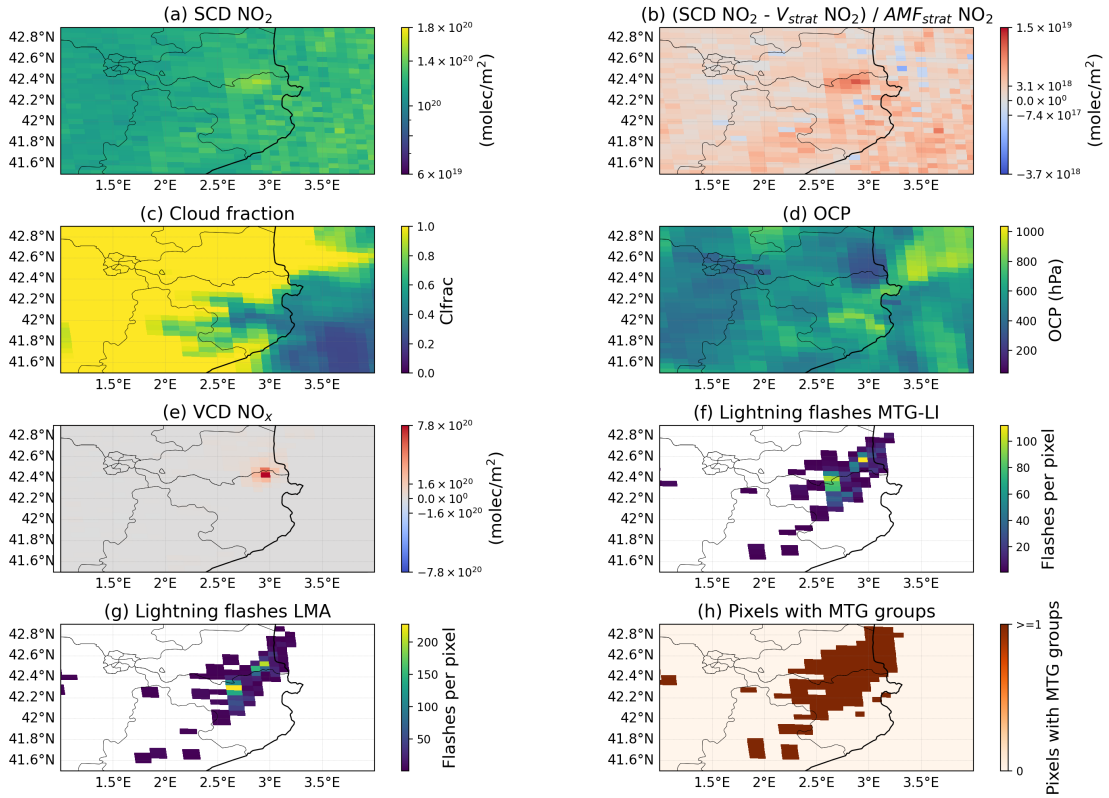

Figure S42. TROP-DLR product of orbit 38890, MTG-LI and LMA lightning data for the case 15 April 2025. (a): Slant Column Density (SCD) of NO_2 provided by the TROP-DLR NO_2 research product. (b): SCD NO_2 minus the stratospheric vertical column density and divided to the stratospheric air mass factor of NO_2 obtained from the TROP-DLR NO_2 research product. (c) and (d): Cloud Fraction (CF) and Optical Centroid Pressure (OCP) from the TROP-DLR NO_2 research product, respectively. (e): VCD of NO_x ($V_{tropNOx}$) over pixels satisfying the DCC. (f) and (g): Lightning flashes during the 5 h period per TROPOMI pixel before the TROPOMI overpass reported by MTG-LI and the LMA, respectively. (h): TROPOMI pixels containing at least one lightning group detected by MTG-LI.

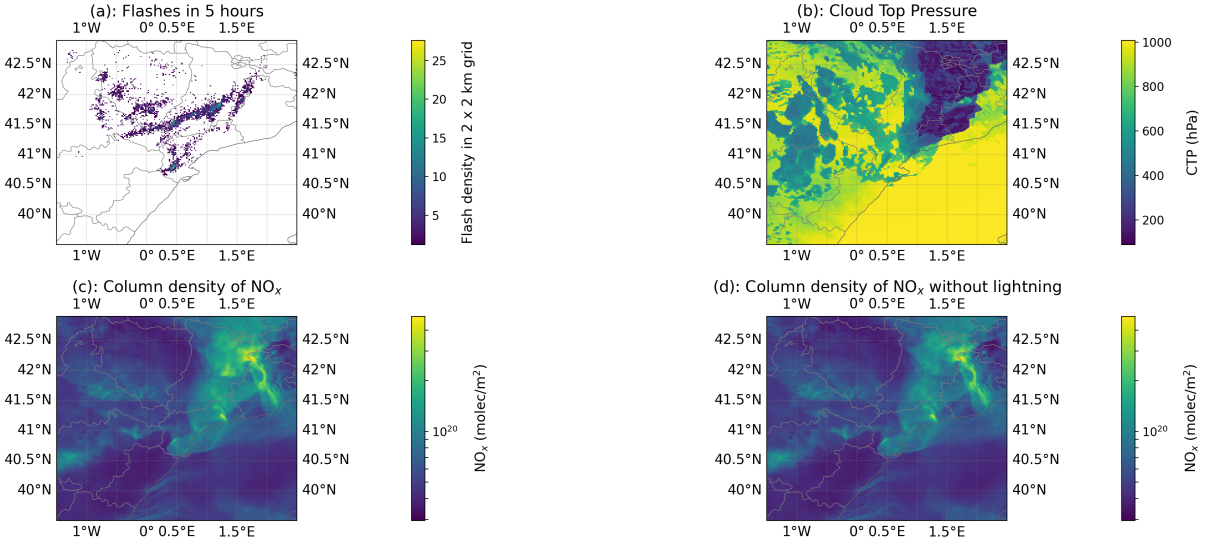

Figure S43. Simulation results for 19 April 2025 at 13:30 UTC, focused on the region of interest. (a): Assimilated lightning flashes between 08:30 and 13:30 UTC reported by MTG-LI. (b): Cloud Top Pressure (CTP). (c): Vertical Column Density of NO_x. (d): Vertical column density of NO_x in the simulation without fresh LNO_x, i.e., with LNO_x deactivated after 07:00 UTC.

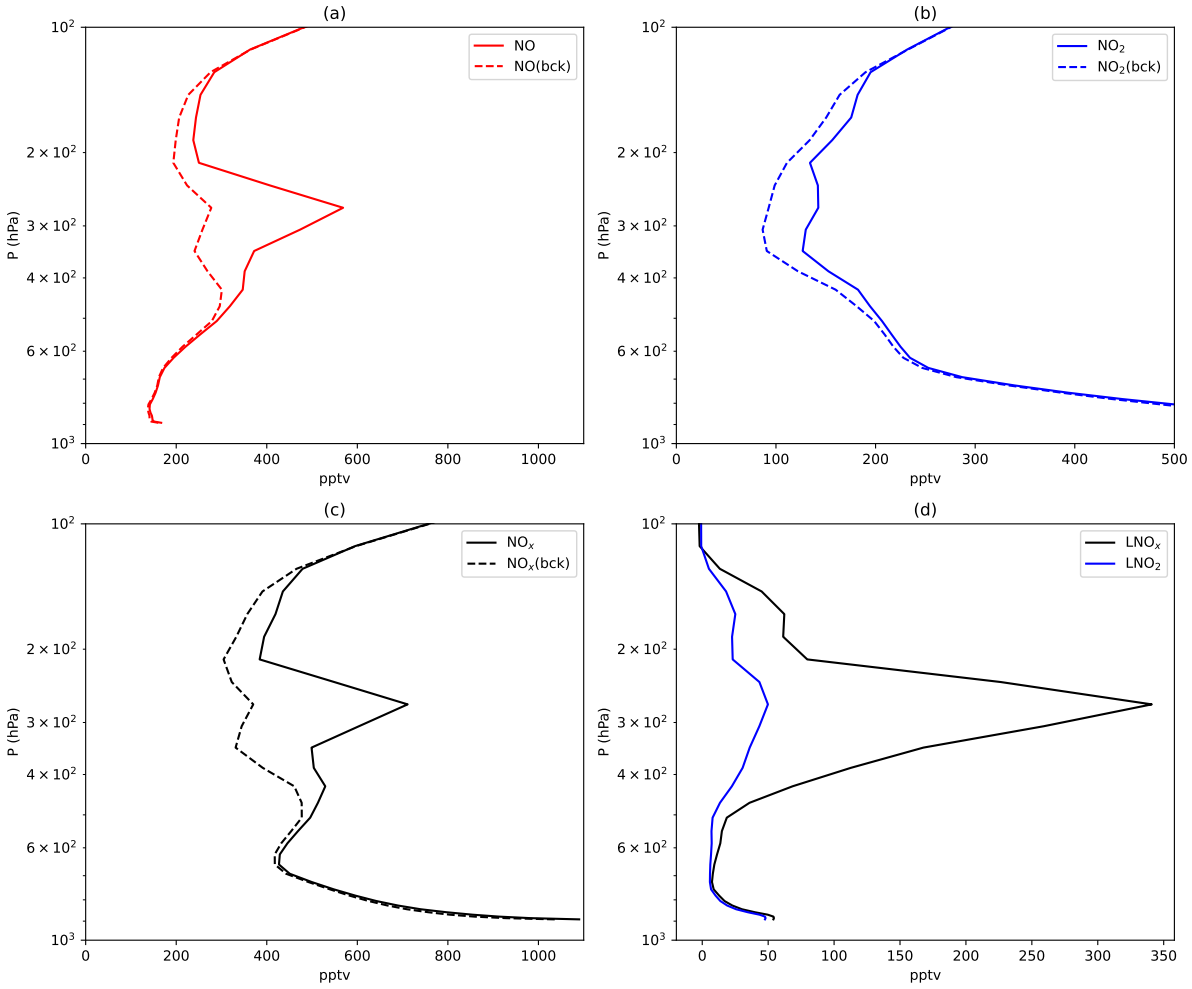

Figure S44. Vertical mixing ratio profiles of NO (a), NO_2 (b), NO_x (c), LNO_x and LNO_2 (d) extracted from WRF-CHEM simulations with (solid lines) and without (dashed lines) fresh LNO_x on 19 April 2025 at 13:30 UTC (close to the TROPOMI overpass (background: bck)).

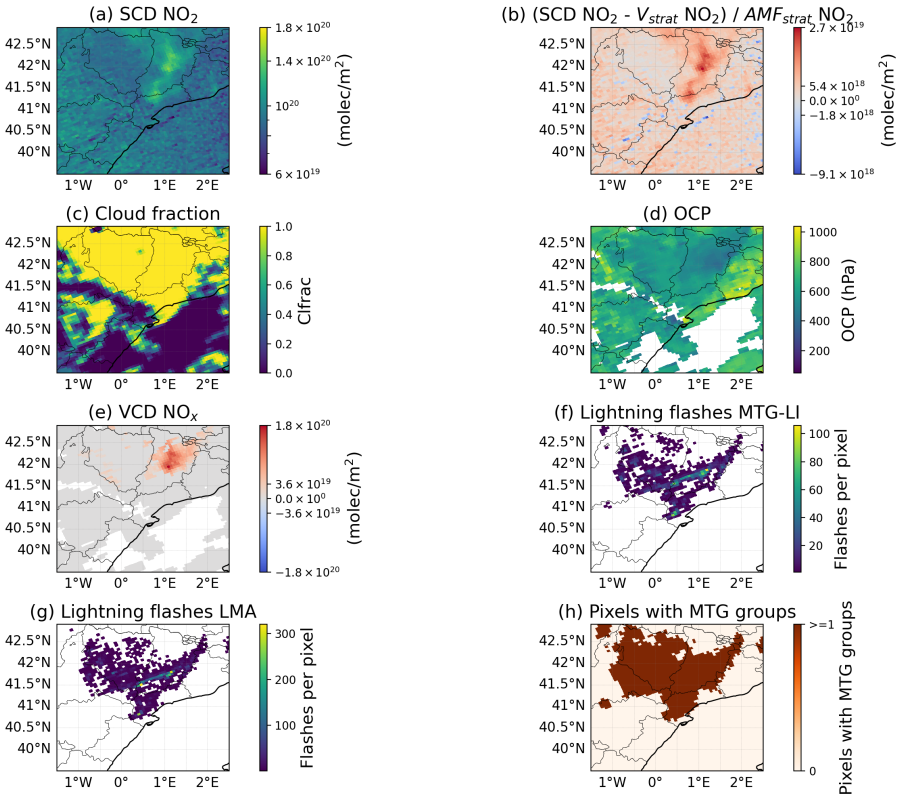

Figure S45. TROP-DLR product of orbit 38946, MTG-LI and LMA lightning data for the case 19 April 2025. (a): Slant Column Density (SCD) of NO_2 provided by the TROP-DLR NO_2 research product. (b): SCD NO_2 minus the stratospheric vertical column density and divided to the stratospheric air mass factor of NO_2 obtained from the TROP-DLR NO_2 research product. (c) and (d): Cloud Fraction (CF) and Optical Centroid Pressure (OCP) from the TROP-DLR NO_2 research product, respectively. (e): VCD of NO_x ($V_{tropNOx}$) over pixels satisfying the DCC. (f) and (g): Lightning flashes during the 5 h period per TROPOMI pixel before the TROPOMI overpass reported by MTG-LI and the LMA, respectively. (h): TROPOMI pixels containing at least one lightning group detected by MTG-LI.

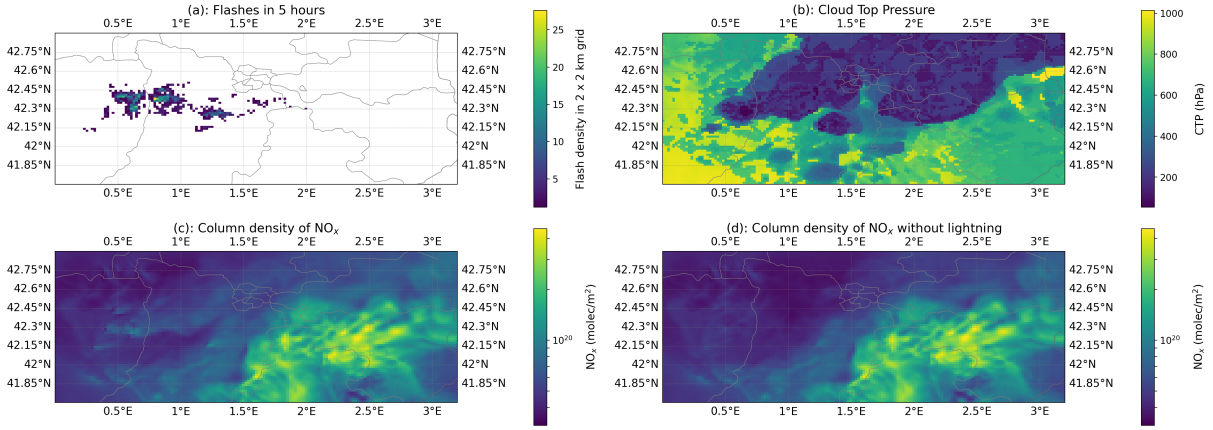

Figure S46. Simulation results for 26 April 2025 at 13:40 UTC, focused on the region of interest. (a): Assimilated lightning flashes between 08:40 and 13:40 UTC reported by MTG-LI. (b): Cloud Top Pressure (CTP). (c): Vertical Column Density of NO_x. (d): Vertical column density of NO_x in the simulation without fresh LNO_x, i.e., with LNO_x deactivated after 07:00 UTC.

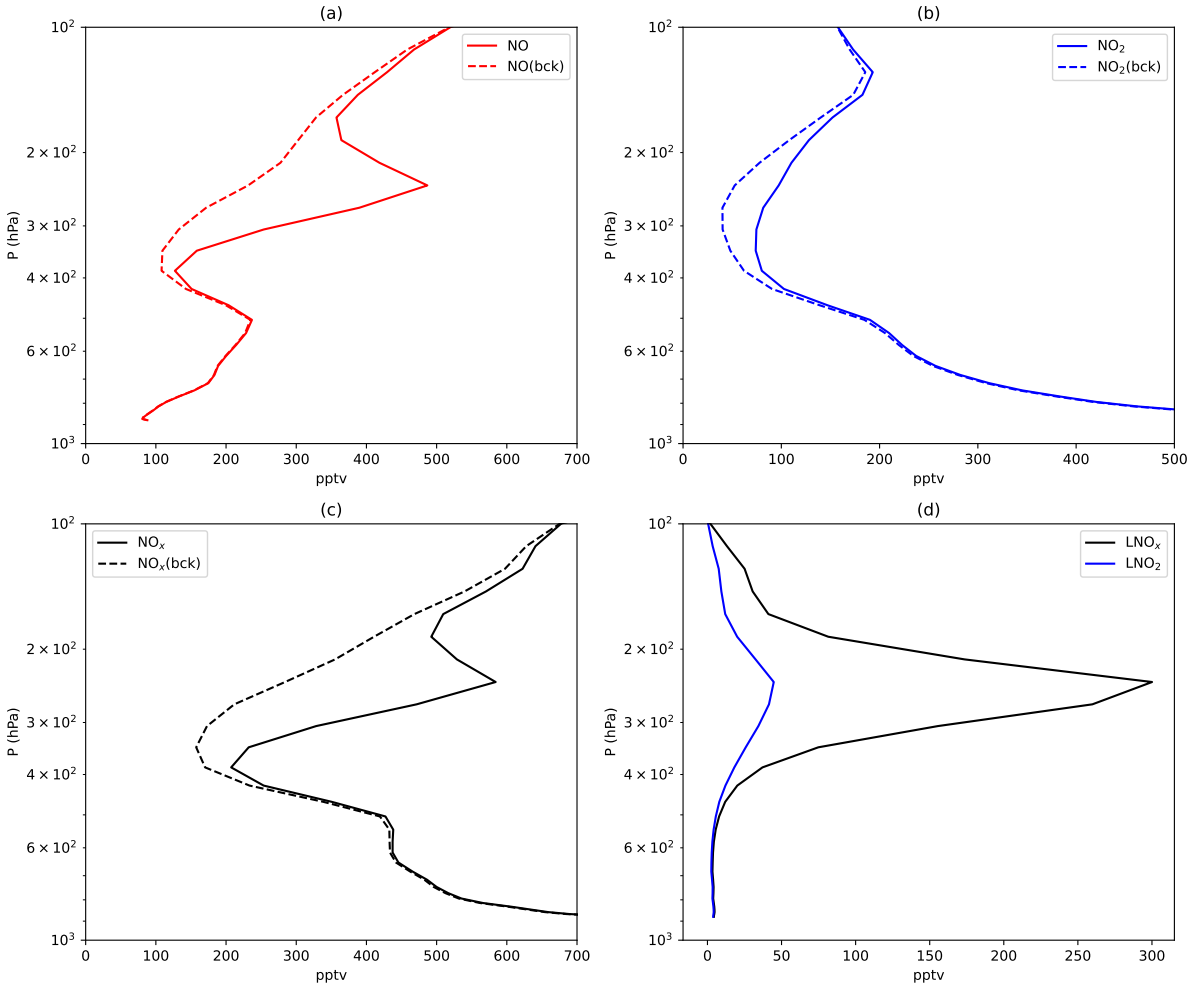

Figure S47. Vertical mixing ratio profiles of NO (a), NO_2 (b), NO_x (c), LNO_x and LNO_2 (d) extracted from WRF-CHEM simulations with (solid lines) and without (dashed lines) fresh LNO_x on 26 April 2025 at 13:40 UTC (close to the TROPOMI overpass (background: bck)).

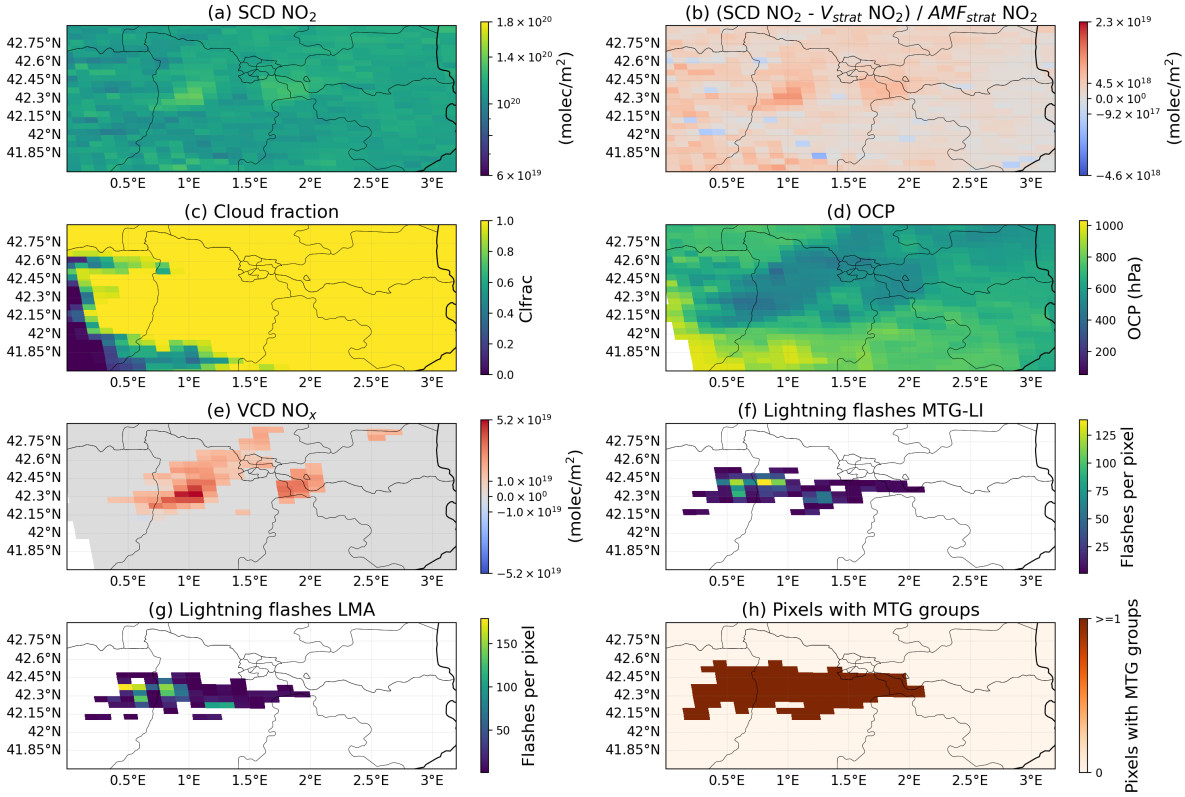

Figure S48. TROP-DLR product of orbit 39046, MTG-LI and LMA lightning data for the case 26 April 2025. (a): Slant Column Density (SCD) of NO_2 provided by the TROP-DLR NO_2 research product. (b): SCD NO_2 minus the stratospheric vertical column density and divided to the stratospheric air mass factor of NO_2 obtained from the TROP-DLR NO_2 research product. (c) and (d): Cloud Fraction (CF) and Optical Centroid Pressure (OCP) from the TROP-DLR NO_2 research product, respectively. (e): VCD of NO_x ($V_{tropNOx}$) over pixels satisfying the DCC. (f) and (g): Lightning flashes during the 5 h period per TROPOMI pixel before the TROPOMI overpass reported by MTG-LI and the LMA, respectively. (h): TROPOMI pixels containing at least one lightning group detected by MTG-LI.

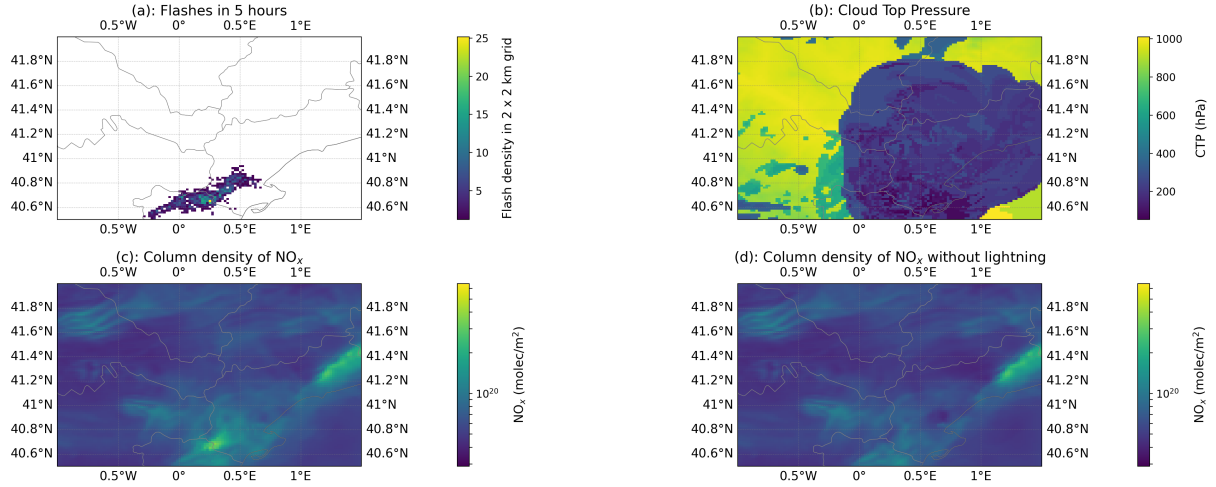

Figure S49. Simulation results for 4 May 2025 at 12:50 UTC, focused on the region of interest. (a): Assimilated lightning flashes between 07:50 and 12:50 UTC reported by MTG-LI. (b): Cloud Top Pressure (CTP). (c): Vertical Column Density of NO_x. (d): Vertical column density of NO_x in the simulation without fresh LNO_x, i.e., with LNO_x deactivated after 07:00 UTC.

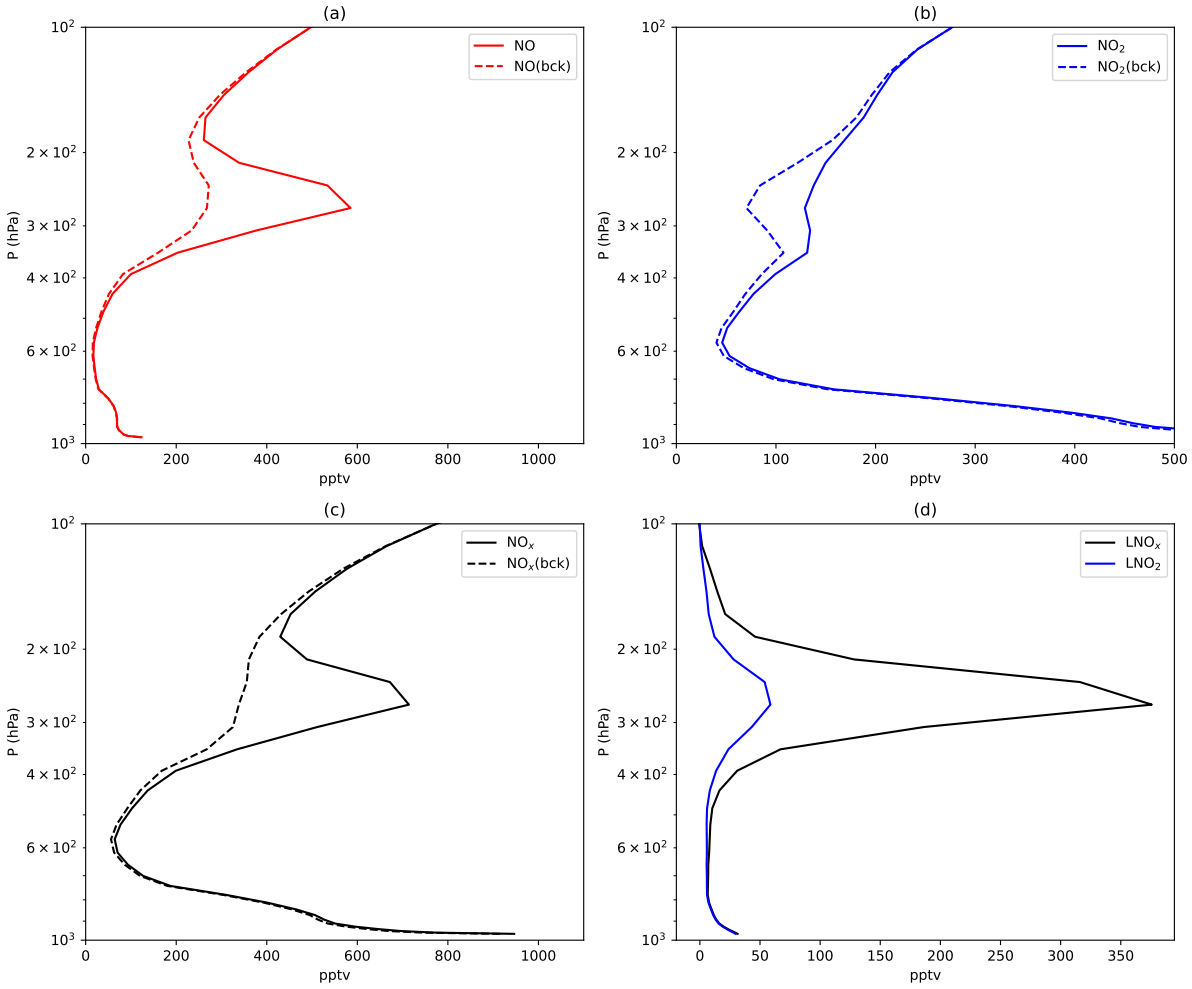

Figure S50. Vertical mixing ratio profiles of NO (a), NO_2 (b), NO_x (c), LNO_x and LNO_2 (d) extracted from WRF-CHEM simulations with (solid lines) and without (dashed lines) fresh LNO_x on 4 May 2025 at 12:50 UTC (close to the TROPOMI overpass (background: bck)).

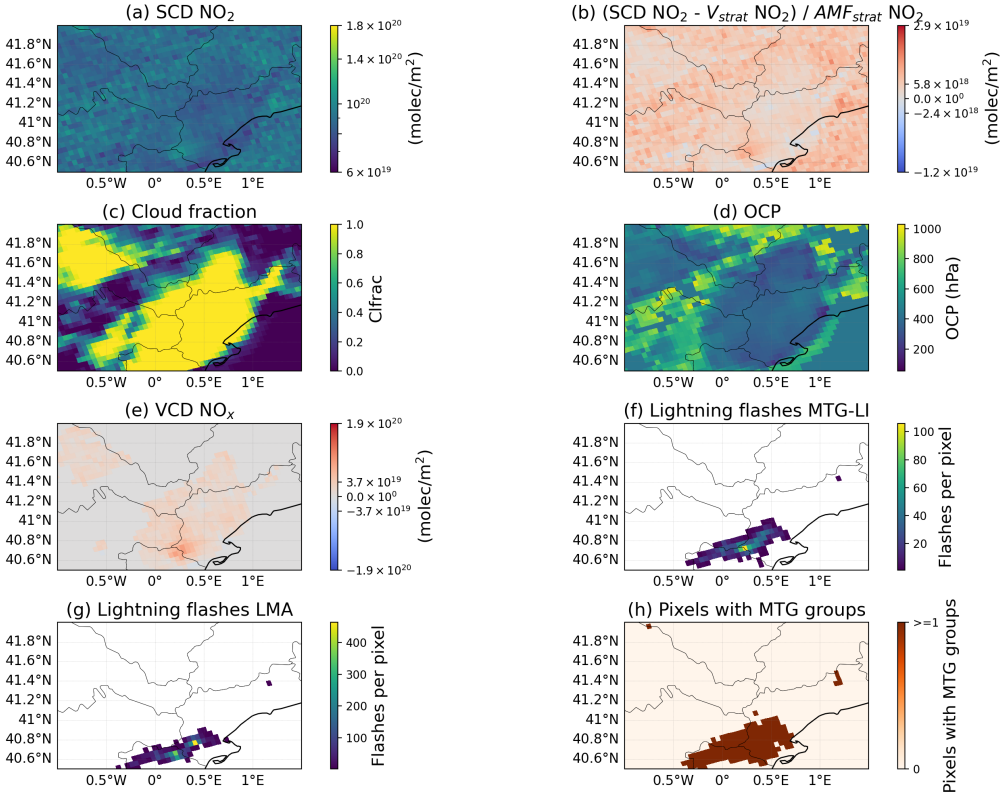

Figure S51. TROP-DLR product of orbit 39159, MTG-LI and LMA lightning data for the case 4 May 2025. (a): Slant Column Density (SCD) of NO_2 provided by the TROP-DLR NO_2 research product. (b): SCD NO_2 minus the stratospheric vertical column density and divided to the stratospheric air mass factor of NO_2 obtained from the TROP-DLR NO_2 research product. (c) and (d): Cloud Fraction (CF) and Optical Centroid Pressure (OCP) from the TROP-DLR NO_2 research product, respectively. (e): VCD of NO_x ($V_{tropNOx}$) over pixels satisfying the DCC. (f) and (g): Lightning flashes during the 5 h period per TROPOMI pixel before the TROPOMI overpass reported by MTG-LI and the LMA, respectively. (h): TROPOMI pixels containing at least one lightning group detected by MTG-LI.

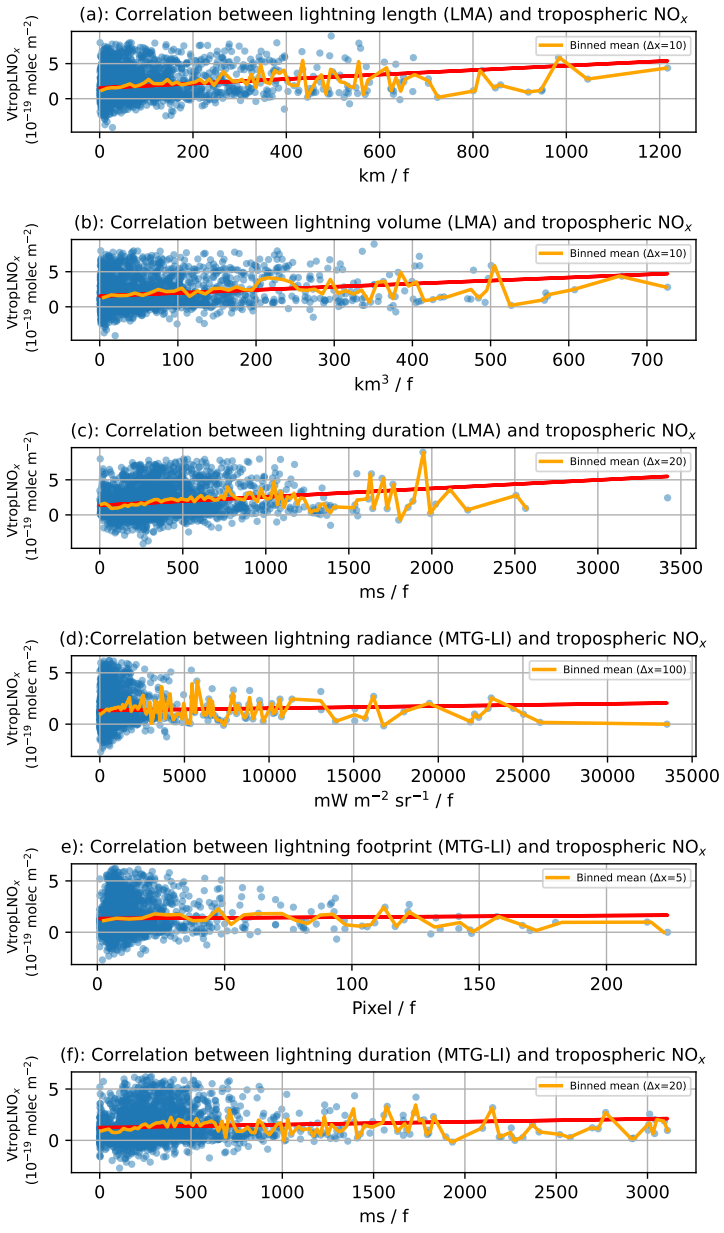

Figure S52. Pixel-based $V_{tropLNOx}$ versus average flash channel lenght (a), average flash volume (b), average flash duration from the LMA (c), average flash footprint (d), average radiance (e) and average flash duration from MTG-LI (f), computed across all pixels included in the 18 analyzed dates. Only pixels with values of $V_{tropLNOx}$ between the 5^{th} and the 95^{th} percentiles are included. The red lines correspond to linear fits of the plotted data, while the orange lines represent binned data obtained by calculating moving averages with a window interval Δx, as indicated in each panel.

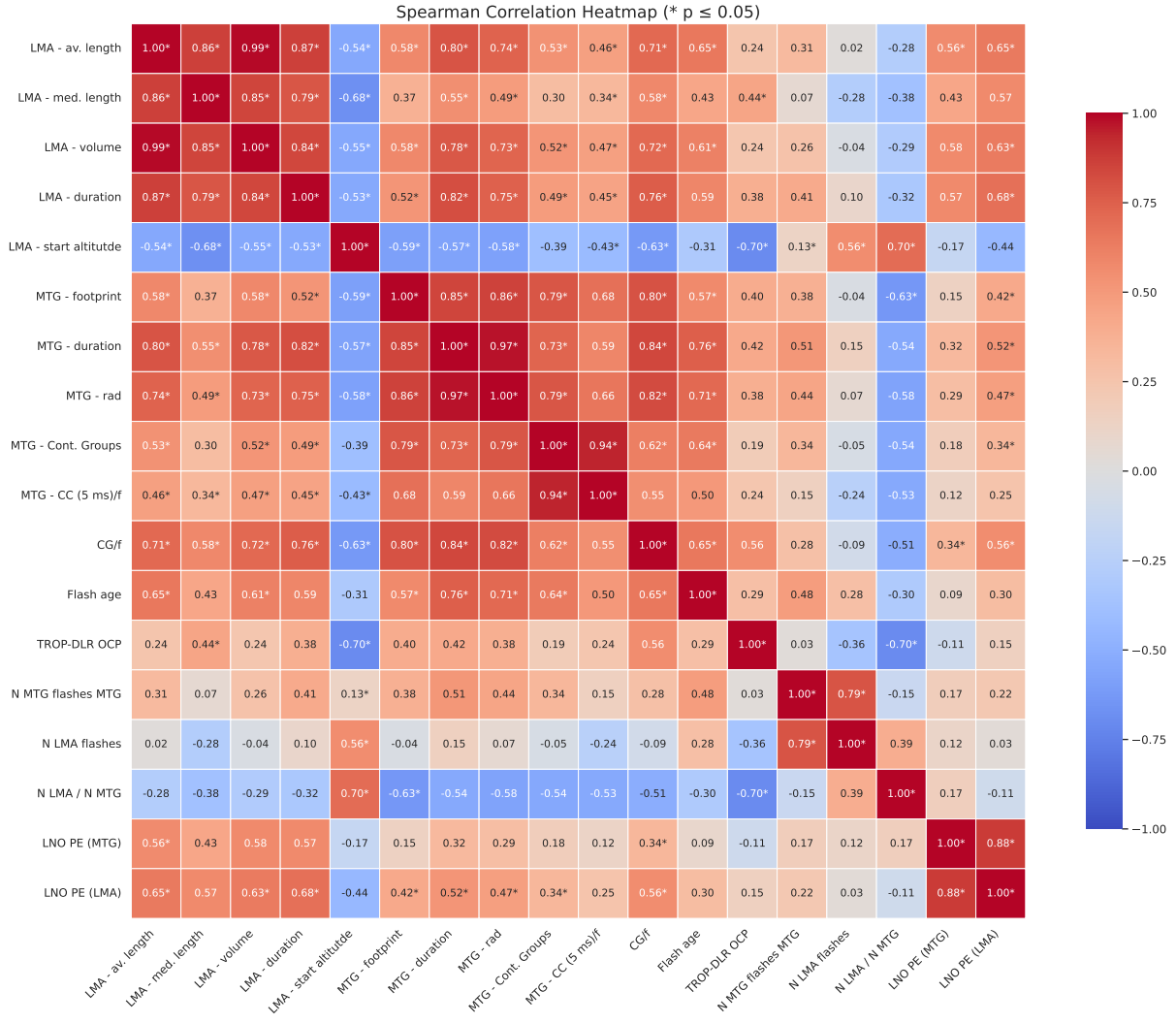

Figure S53. Spearman correlation heatmap of the most important lightning characteristics and LNO_x PE estimates. These results are based on caculations with $\tau = 3$ h.

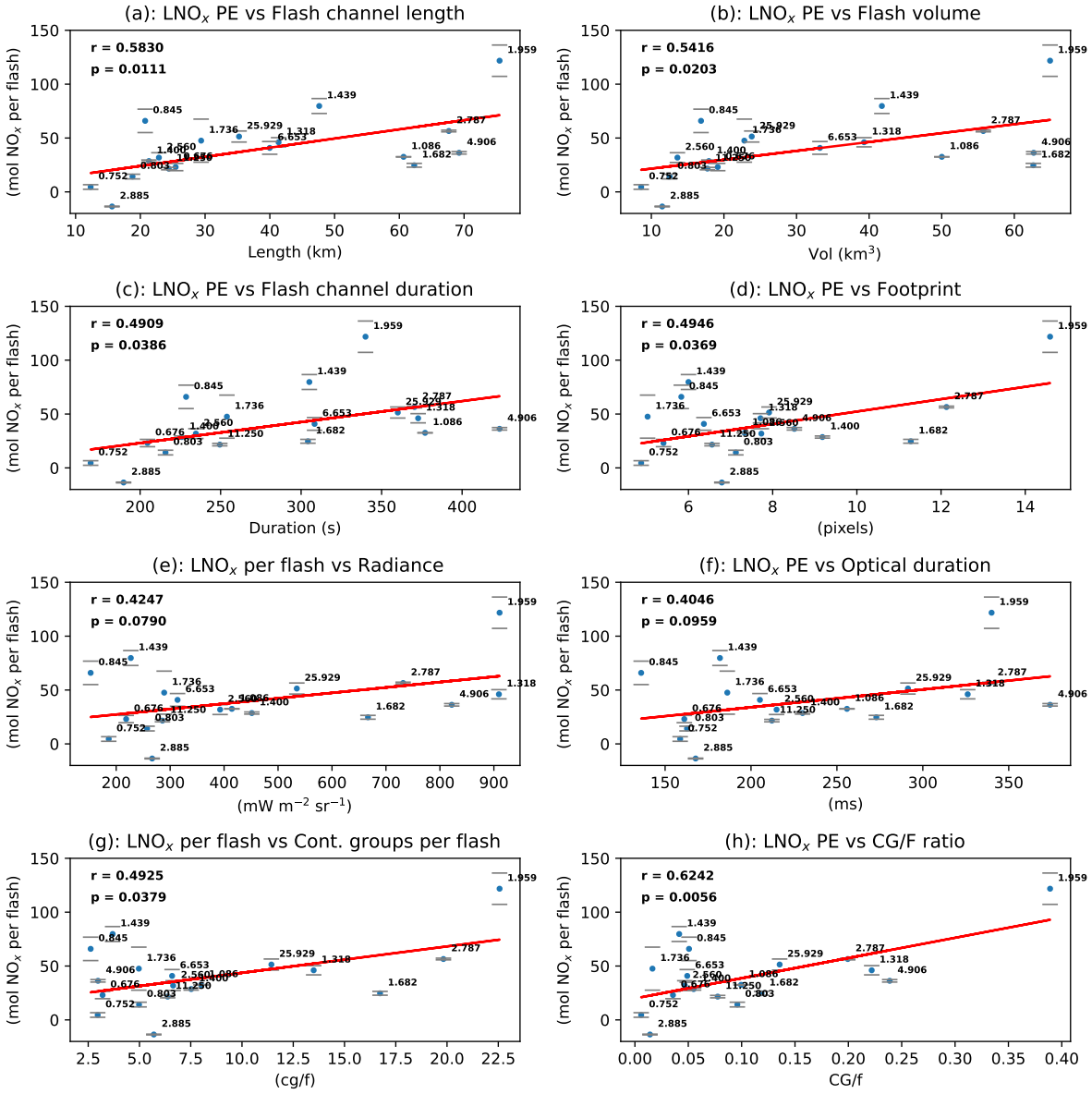

Figure S54. Pearson correlation between the LNO$_x$ PE and the most important lightning characteristics included in this study. The average LNO$_x$ PE (blue points) is obtained as the average between the LNO$_x$ PE estimates by using both MTG-LI and the LMA for each analyzed case, while each pair of grey bars are the values of the LNO$_x$ PE estimates by using MTG-LI and the LMA separately. The numbers close to the points represent the total number of flashes reported by MTG-LI in units of kfl. The flash channel length, the flash volume and the flash durations in panels (a), (b) and (c) are the average values calculated from LMA measurements. The footprint, the radiance, the flash durations and the total number of contiguous groups per flash in panels (d), (e), (f) and (g) are the average values calculated from MTG-LI measurements. The average ratio of CG to total flashes in panel (h) is obtained from LLS-SMC and LMA lightning measurements. Each subplot includes the Pearson correlation coefficient r and its corresponding $p-value$, as well as a linear fitting of the blue points (red line). These results are based on caculations with τ = 3 h.

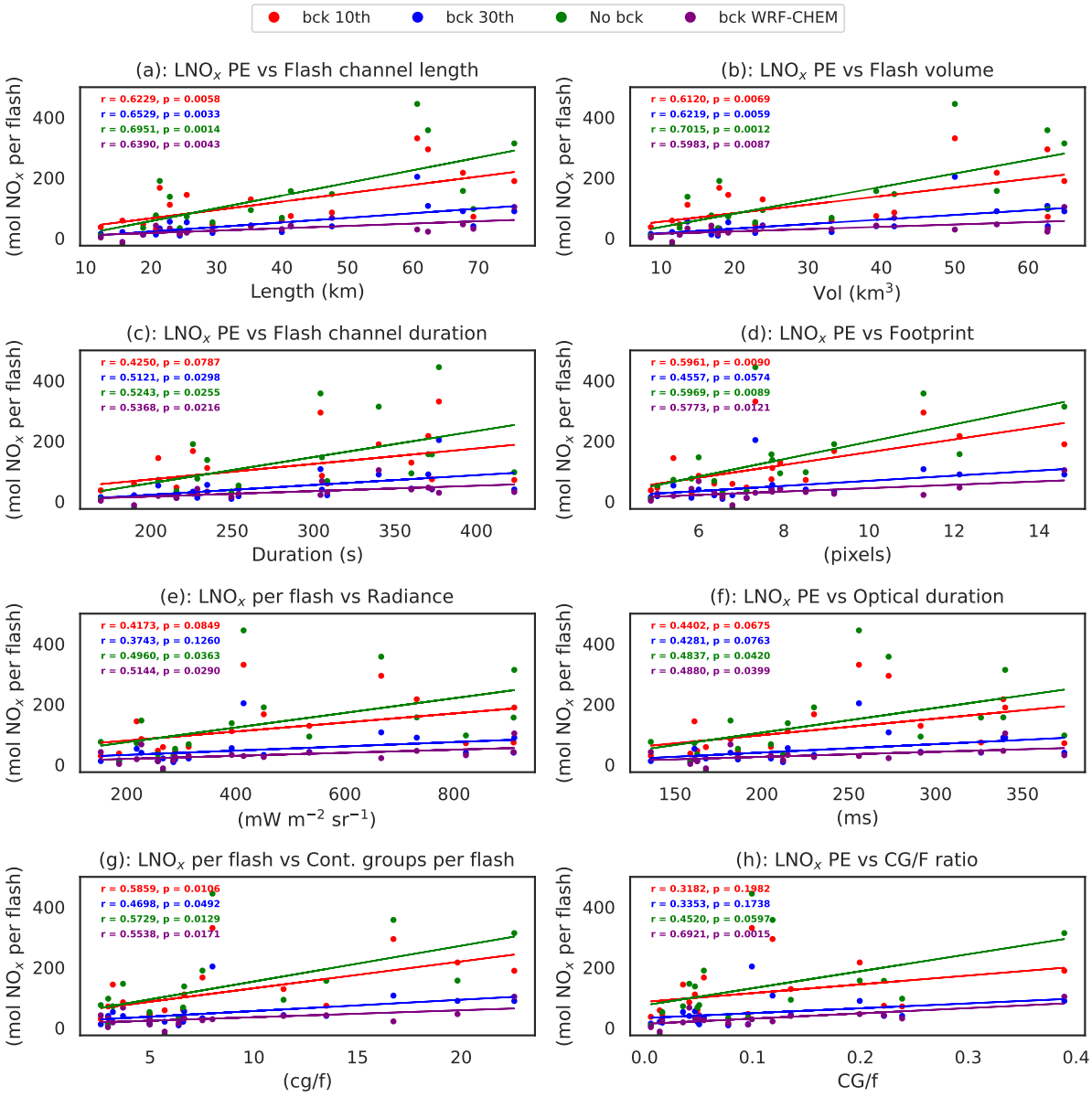

Figure S55. Analysis of the influence of the background-NO$_x$ estimate in the obtained relationships. This plot shows the pearson correlation between the LNO$_x$ PE and the most important lightning characteristics included in this study by assuming that the background-NO$_x$ is the 10th percentile (red), the 30th percentile (bue) of the VCD tropospheric NO$_x$ over non-flashing pixels, without substracting the background-NO$_x$ (green), and using the WRF-Chem simulations (purple) to calculate the background-NO$_x$. The LNO$_x$ PE is obtained as the LNO$_x$ PE estimates by using the LMA for each analyzed case. The flash channel length, the flash volume and the flash durations in panels (a), (b) and (c) are the average values calculated from LMA measurements. The footprint, the radiance, the flash durations and the total number of contiguous groups per flash in panels (d), (e), (f) and (g) are the average values calculated from MTG-LI measurements. The average ratio of CG to total flashes in panel (h) is obtained from LLS-SMC and LMA lightning measurements. Each subplot includes the Pearson correlation coefficient r and its corresponding $p-value$, as well as a linear fitting of the blue points (solid lines). These results are based on caculations with τ = 5 h.

15 *Competing interests.* Authors declare no competing interests.